[illegible]

NATIONAL ADVISORY COMMITTEE FOR AERONAUTICS

TECHNICAL NOTE

No. 1202

MEASUREMENTS OF THE PRESSURE DISTRIBUTION ON THE HORIZONTAL TAIL SURFACE OF A TYPICAL PROPELLER-DRIVEN PURSUIT AIRPLANE IN FLIGHT

II - THE EFFECT OF ANGLE OF SIDESLIP AND PROPELLER OPERATION

By Melvin Sadoff and Lawrence A. Clousing

Ames Aeronautical Laboratory

Moffett Field, Calif.

LIBRARY COPY

2 1993

LANGLEY RESEARCH CENTER
LIBRARY NASA
HAMPTON, VIRGINIA

Washington

May 1947

3 1176 01433 9007

NATIONAL ADVISORY COMMITTEE FOR AERONAUTICS

TECHNICAL NOTE NO. 1202

MEASUREMENTS OF THE PRESSURE DISTRIBUTION ON THE HORIZONTAL TAIL SURFACE OF A TYPICAL PROPELLER-DRIVEN PURSUIT AIRPLANE IN FLIGHT

II – THE EFFECT OF ANGLE OF SIDESLIP AND PROPELLER OPERATION

By Melvin Sadoff and Lawrence A. Clousing

SUMMARY

Measurements were made in sideslipping flight at a Mach number of 0.50 of the pressure distribution over the horizontal tail surfaces of a tractor-propeller-driven pursuit airplane, to determine the effects of angle of sideslip and propeller operation on the tail-load distribution. Measurements were also made of the tail-load distribution on the horizontal tail in steady unaccelerated flight over a Mach number range of 0.30 to 0.79 and 0.30 to 0.74, respectively, for the power-on and power-off conditions.

It is shown that the asymmetric tail loading results from a large decrease in load on the blanketed tail and a small increase of load on the leading tail. Although, in general, the application of power at a speed of 290 miles per hour results in an increase in the positive asymmetric loading over the sideslip-angle range, the effect is relatively small as compared with that of sideslip angle. The asymmetric loads and torsional moments at low speeds and zero angle of sideslip are small and unimportant even with power on. At high speeds in sideslipping flight, the total fuselage torsion may become critical since the torsional moment due to asymmetric tail loading is in the same direction as that resulting from vertical-tail loads. Critical bending moments may occur in left sideslip on the left tail at moderate speeds and at the limit load factor if the computed up-load does not include the increments in up-load due to both propeller operation and angle of sideslip. The greater negative total tail loads associated with an increase in sideslip angle may result in critical balancing down-loads at high speeds because of the initially high down-loads required to balance the airplane at zero sideslip.

Comparison of the results with limit values computed on the basis of current Army specifications indicated that the calculated values of asymmetric tail load and the resultant fuselage torsional moment are conservative as compared with the experimental results for critical flight conditions. The calculated root bending moment, however, may be unconservative by as much as 25 percent as compared with the actual value for critical flight conditions.

INTRODUCTION

Numerous structural failures of the tail surfaces of high-speed military aircraft have occurred within recent years indicating a possible need for modifying the existing design specifications. In order to determine in what respects existing requirements were inadequate and to provide data as a basis for any revisions or modifications deemed necessary, an extensive tail-load investigation was conducted on a typical tractor-propeller-driven pursuit airplane, in flight. Pressure distribution measurements were made on the horizontal tail in steady unaccelerated flight $(A_Z = 1.0)$, steady accelerated flight, steady sideslips, and abrupt maneuvers. Results of the tests made in steady unaccelerated and steady accelerated flight are reported in reference 1. This report, the second of a series, presents the results obtained in steady sideslips, (as measured in gradual dive pull-outs), and shows the changes in horizontal-tail loading that occur as a result of propeller operation and angle of sideslip. The asymmetric load, the root bending moment, and the torsional moment, computed by the methods specified in the current Army design requirements, are compared with the experimental values at critical conditions.

SYMBOLS

The following symbols are used in this report:

M	free-stream Mach number
V_i	correct indicated airspeed $\left\{1703\left[\left(\frac{H-p}{p_o}+1\right)^{0.286}-1\right]^{\frac{1}{2}}\right\}$, miles per hour
H	free-stream total pressure
p	free-stream static pressure
p_o	standard atmospheric pressure at sea level

h_p	pressure altitude, feet
C_L	airplane lift coefficient $\left(\frac{W\ A_Z}{q\ S_w}\right)$
W	average airplane weight during test run, pounds
A_Z	the ratio of the net aerodynamic force along the airplane Z-axis (positive when directed upward) to the weight of the airplane
q	free-stream dynamic pressure, pounds per square foot
S	horizontal-surface area, square feet
b_t	horizontal-tail span, feet
N_t	total air load on horizontal tail $(N_{t_L} + N_{t_R}$, positive when load is acting upward), pounds
N_{tA}	asymmetric tail load $(N_{t_L} - N_{t_R})$, pounds
M_T	torsional moment on fuselage due to horizontal-tail loading (positive when moment is clockwise as seen from rear), pound-feet
M_r	root bending moment (positive when moment is clockwise as seen from rear), foot-pounds
C_{M_T}	torsional-moment coefficient $\left(\frac{M_T}{qS_tb_t}\right)$
C_{N_t}	tail normal-force coefficient $\left(\frac{N_t}{qS_t}\right)$
C_{M_r}	root bending-moment coefficient $\left(\frac{M_r}{qS_tb_t}\right)$
c_n	section normal-force coefficient
c	local tail chord, feet
p_u	pressure on upper surface, pounds per square foot
p_l	pressure on lower surface, pounds per square foot
P_{RES}	resultant pressure coefficient $\left(\frac{p_l - p_u}{q}\right)$

Q	propeller torque, pound-feet
Q_c	propeller-torque coefficient $\left(\frac{Q}{2qD^3}\right)$
T	propeller thrust, pounds
T_c	propeller-thrust coefficient $\left(\frac{T}{2qD^2}\right)$
D	propeller diameter, feet
$\Delta C_{N_{t_A}}$	$\left[C_{N_{t_A}(\text{power on})} - C_{N_{t_A}(\text{power off})}\right]_{C_L}$
ΔC_{M_T}	$\left[C_{M_T(\text{power on})} - C_{M_T(\text{power off})}\right]_{C_L}$
ΔQ_c	$\left[Q_{c(\text{power on})} - Q_{c(\text{power off})}\right]_{C_L}$
δ_e	elevator angle (positive when trailing edge is down), degrees from thrust axis
β	sideslip angle (positive when right wing is forward), degrees

Subscripts

w	wing
t	horizontal tail
L	left
R	right
A	asymmetric

DESCRIPTION OF AIRPLANE

The test airplane is a single-engine, interceptor-pursuit, low-wing monoplane driven by a tractor propeller and equipped with a retractable tricycle landing gear. Figures 1 and 2 are photographs of the airplane as instrumented for the flight tests; figure 3 is a three-view drawing of the airplane. Pertinent specifications of the horizontal tail surfaces are as follows:

Span, ft	13.0
Area, sq ft	40.99
Airfoil section	NACA approx. 0010 to 0006 (fig. 4 of reference 1)
Stabilizer setting (relative to airplane thrust axis), deg.	2.25
Elevator area (including 4.3 sq ft overhang balance), sq ft	16.89
Nominal deflection	35° up, 15° down
Dihedral angle, deg	0

Further detail specifications of the test airplane may be obtained from reference 1.

INSTRUMENTATION AND PRECISION

A 60-cell pressure recorder located in the rear section of the fuselage between the oil tank and the baggage compartment was used to measure the resultant pressures over the horizontal tail at the locations given in table I and shown in figure 4. The precision with which the pertinent quantities were believed to be measured in the tests is indicated in the following table:

Item	Estimated precision
Normal acceleration	±0.05g
Elevator angle	±0.50°
Sideslip angle	±1.0°
Airspeed (to 200 mph)	±2½ percent
(above 200 mph)	±1½ percent
Altitude	±300 feet
Tail load (low speeds, unaccelerated flight)	±50 pounds
(high speeds, accelerated flight)	±100 pounds

The pressure-lag characteristics of typical horizontal tail lines were investigated, and it was found that the lag was negligible for the rates of pressure change encountered in this investigation. Other instrumentation of the test airplane and the precision of the measurements were the same as given in reference 1.

FLIGHT PROGRAM

With normal rated power (39 in. Hg and 2600 rpm) at a pressure altitude of 15,000 feet and at an indicated airspeed of 290 miles per hour, runs were made at sideslip angles of approximately 0°, 5° left, 10° left, 5° right, and 10° right. All these tests were performed by pulling out gradually from a shallow dive while attempting to maintain the sideslip angle requested. Tests were repeated, power off, with the engine fully throttled and the propeller in high pitch.

Tests, which were made for obtaining data given in reference 1, were also used for the present report. The tests used were those run in steady unaccelerated flight with wings level, power on, full throttle and 3000 rpm at a pressure altitude of 15,000 feet and at indicated airspeeds ranging from 170 to about 460 miles per hour. Tests were repeated, power off, with the indicated airspeed varying from 170 to about 430 miles per hour.

Curves taken from reference 2 showing the variation of brake horsepower (as determined by reference to engine power charts) with pressure altitude, and the variation of propeller-blade angle and engine speed with true airspeed are shown in figure 5 for the engine power settings used for these tests.

All tests were made with the center of gravity located at 30.3 percent of the mean aerodynamic chord.

RESULTS AND DISCUSSION

Reduction of Data

Although the results presented in this report were obtained in gradual dive pull-outs, they are treated as though obtained in steady sideslips. This is felt to be justified since the positive pitching accelerations during the pull-outs were small, and no consistent relationship was found between the scatter in the data and the magnitude of the negative pitching accelerations obtained during recovery from the pull-outs.

In the analysis of the data referred to in reference 1 and in the subsequent discussion and analysis in this report, the term "steady unaccelerated flight" denotes steady flight at a normal acceleration of 1g. It is believed that this use is justified even at diving speeds because the magnitude of pitching velocity necessary to result in a normal acceleration of 1g was negligible.

Chordwise and spanwise loading.- The resultant pressure coefficients for each orifice station were plotted against tail chord for selected time points during each test run to obtain the chordwise distribution of the tail load. Mechanical integration of the chordwise loading gave the variation of load c_nc across the tail span. Some typical chordwise and spanwise distributions are shown in figures 6 and 7. These figures present the power-on and power-off pressure distributions, respectively, at maximum left, zero, and maximum right sideslip angles for lift coefficients of approximately 0.20 and 0.80. The effects of sideslip angle and power may be readily seen by comparing corresponding distributions in figures 6 and 7.

Time histories of pertinent variables.- The normal-force coefficients and root bending-moment coefficients for each side of the tail were determined by integrating the spanwise distributions of c_nc. Selected time histories of these coefficients and the derived asymmetric-load and torsional-moment coefficients are presented in figures 8 and 9. Also included in these figures are time histories of other pertinent quantities such as elevator angle, sideslip angle, lift coefficient, acceleration factor, and indicated airspeed. Figure 8 shows the power-on data for runs in which sideslip angles of 12.3°, -2.2°, and -6.4° were attained at the time that the maximum normal acceleration was reached. The power-off data are presented in figure 9 for sideslip angles of 10.5°, 0.7°, and -12.0°. From figures 8 and 9, and similar figures not included in this report, most of the subsequent figures were derived.

Effect of Sideslip and Power on Tail Loads

Left- and right-tail loads.- At time points corresponding to lift coefficients of 0.20, 0.40, 0.60, and 0.80 the values of left- and right-tail normal-force coefficients were determined for each test run and plotted against the corresponding values of sideslip angle. (See fig. 10.) There is considerable scatter of data presented in figure 10 and in a subsequent figure similarly derived (fig. 18), especially for the power-off data at the higher lift coefficients. This probably results from the fact that since some of the pull-outs were not made as gradually as others (figs. 8 and 9), the accuracy with which the times were coordinated for the different instrument records varied from run to run.

It is clearly seen in figure 10 that the leading tail experiences relatively small changes in normal-force coefficient as the sideslip angle is increased, while considerable decreases of load on the blanketed tail are noted. Since these unsymmetrical changes of normal-force coefficient are similar for both the power-on and power-off conditions, it appears that changes in air flow over the horizontal tail due to the yawed fuselage and vertical tail are the principal factors effecting these changes of load with sideslip. An analysis of the leading-edge pressures for the power-on and power-off conditions showed the existence of a strong localized downwash field extending over about 2 feet of span. At zero sideslip angle this field was centered approximately at the fuselage center line and, as the sideslip angle was increased in either direction, moved progressively outboard on the trailing tail. The location appeared to be independent of both power and lift coefficient at the test speed, since with increasing sideslip angle the downwash field moved outboard of the fuselage center line approximately the same amount for all the test conditions. Unfortunately, the data were insufficient to permit quantitative application of these results. A cross plot of the values in figure 10 was made so that the power-on and power-off results could be more readily compared. Figure 11, which resulted, shows the variation of left- and right-tail normal-force coefficients with lift coefficient at several angles of sideslip. Although the power effects are not large because of the low values of thrust coefficient and torque coefficient (about 0.016 and 0.008, respectively, at an indicated speed of 290 mph), the application of power resulted, in general, in higher positive load coefficients on the left tail and lower positive values on the right tail over the sideslip-angle range tested.

Total tail loads.- The variation with sideslip angle of the total tail normal-force coefficient presented in figure 12 was obtained by combining the left and right normal-force coefficients shown in figure 10. The decrease in the value of C_{N_t} indicates an increase in the nose-down pitching moment of the airplane without tail as the sideslip angle was increased in either direction.

The data in figure 14(a) of reference 1 showed a trend toward critical balancing down-loads on the tail at high Mach numbers, and the data of this report (fig. 12) indicate that increasing down-loads for balance were required as the sideslip angle was increased. Therefore, the variation of total tail load with sideslip angle at several values of lift coefficient for steady unaccelerated flight ($A_Z = 1.0$) was determined by combining these data. The validity of the curves is based on the assumption that the slope of the curve of pitching-moment coefficient versus sideslip angle for the test airplane with tail off does not change with Mach number. The three curves in figure 13 are given for the highest power-on and power-off test speeds in reference 1 ($V_i = 463$ mph; $C_L = 0.069$; $V_i = 428$ mph; $C_L = 0.080$, respectively) and for the test speed at which sideslip data were obtained (V_i = 290 mph; C_L = 0.171). The data for the highest speed (M = 0.79; C_L = 0.069) in figure 13 indicate that about 850 pounds greater down-load is required for balance at either 10° left or right sideslip than at zero sideslip.

Asymmetric loads.- The faired curves presented in figure 10 were combined in figure 14 to give the variation of asymmetric-load coefficient with sideslip angle at two values of lift coefficient. As expected, at zero angle of sideslip, the power-on asymmetric-load coefficients were more positive than the power-off coefficients. The difference between power-on and power-off coefficients, however, tended to decrease with increasing sideslip, particularly at large angles of right sideslip. Figure 14 also shows that the highest asymmetric-load coefficients were obtained at the lower values of lift coefficient, more so in right than in left sideslip.

The variation of asymmetric-load coefficient with lift coefficient in steady unaccelerated flight (fig. 15), and the variation with indicated airspeed of asymmetric load (fig. 16) were derived from the data compiled in reference 1. These figures show that there was a decrease in asymmetric load with speed corresponding to a decrease in power effects (slipstream rotation) up to an indicated airspeed of about 380 miles per hour (C_L = 0.10). At higher speeds the asymmetric loads increased rapidly indicating that other factors besides power were affecting the tail-load asymmetry.

The variation of asymmetric loads with sideslip angle for several values of lift coefficient in steady unaccelerated flight, as shown in figure 17, was determined from the power-on data in figures 14 and 15. The use of curve for C_L = 0.20 in figure 14 at higher speeds is based on the assumptions that (1) Mach number effects on the slope of the $C_{N_{t_A}}$ versus β curve were negligible and (2) C_L and power had no appreciable effect on the slope of the $C_{N_{t_A}}$ versus β curve at level flight speeds higher than that corresponding to C_L = 0.20. The data of reference 3 showed the latter assumption was justified. In figure 17 it is shown that the maximum asymmetric load will occur at high speeds and in left sideslip. The asymmetric loads at low speeds (C_L = 0.171 and higher) are relatively small and unimportant.

Effect of Sideslip and Power on Tail Moments

Tail root bending moments.- The variation of the left- and right-tail root bending-moment coefficients with sideslip angle was determined for several values of lift coefficient and is presented in figure 18. Corresponding to similar variations in normal-force coefficient, the data show that as the sideslip angle was increased marked changes in tail loading occurred only for the blanketed side of the tail, while the leading tail experienced only a slight increase in root bending moment. The right-tail root bending moments, however, started to decrease at angles of right sideslip above about 5°, particularly for the power-off condition.

A cross plot of figure 18 showing the variation of left- and right-tail root bending-moment coefficients with lift coefficient for several angles of sideslip is presented as figure 19. In general, the effect of power was to increase the left-tail moments and decrease the right-tail moments except in the case of the blanketed tail at high sideslip angles where the power effects disappeared or reversed.

Faired curves in figure 20, which show the variation of lateral center of pressure on the horizontal tail with side-slip angle, were obtained by combining the curves of figures 10 and 18 for a lift coefficient of 0.80. For positive loads on the tail there was a tendency for the center of pressure to move outboard as the lift-coefficient was decreased; nevertheless, this was not considered a critical trend toward maximum bending moments, since the tail loads would not be a maximum for the same conditions for which the center-of-pressure distance was a maximum. Figure 20 shows that as the sideslip angle was increased, the center of pressure moved inboard on the blanketed tail while it remained practically constant on the leading tail. Therefore, at high angles of sideslip, greater bending moments than those predicted assuming symmetrical loading may be experienced by the leading tail due to the increased loads.

Fuselage torsional moments.- The variation of fuselage torsional-moment coefficient with sideslip angle for two values of lift coefficient (fig. 21) was obtained by combining the values of left- and right-tail root bending-moment coefficients in figure 18. It is shown that the effect of power was to increase the positive torsional moment at all except the highest angles of right sideslip. It is apparent that changing C_L in the constant-speed accelerated flight had no appreciable effect on the fuselage torsional moment.

The torsional-moment coefficients for several values of lift coefficient in steady unaccelerated flight in figure 22 and the variation of torsional moment with indicated speed in steady unaccelerated flight in figure 23 were derived from the data of reference 1. As previously noted for the asymmetric loads, power effects, which resulted in positive torsional moments, diminished with increasing speed up to a speed of about 380 miles per hour ($C_L = 0.10$). Above 380 miles per hour, the torsional moments became more positive with increasing speed more so with power on than with power off. Figure 24 shows that the torsional moment and asymmetric-load coefficients were proportional mainly to power (slipstream rotation) up to speeds corresponding to a ΔQ_c of about 0.010. At higher speeds, power resulted in only secondary effects on C_{M_T} and $C_{N_{t_A}}$.

From the power-on data given in figures 21 and 22, the variation of torsional moment with sideslip angle for several values of lift coefficient in steady unaccelerated flight was obtained. Although the slopes of the curves in figure 21 are for a T_c of about 0.016, their use at higher speeds (and lower T_c's) does not entail appreciable error because of the relatively small changes in T_c and Q_c at speeds higher than 290 miles per hour. The results presented in figure 25 show that the maximum fuselage torsional moment will occur during a high-speed pull-out when appreciable sideslip may be inadvertently developed. The torsional moments at indicated speeds of 290 miles per hour or lower $(C_L \geqq 0.171)$ are relatively small and unimportant.

Comparison of the Calculated Loading with Experimental Results

Current Army design specifications require that, "the horizontal tail surfaces, attachment fittings, and carry-through structure shall be designed for an unsymmetrical load condition where the load on one side is the maximum load for that side obtained from any condition while the load on the other side is the load from the foregoing condition multiplied by the factor $\left(1 - \frac{n}{7.33}\right)$ where n is the limit maneuvering load factor for which the airplane is designed." The condition for which maximum loads would be experienced was determined from reference 4 where it was shown that the maximum maneuvering load (an up-load) would be encountered at sea level and at a speed corresponding to the upper left-hand corner of the V-g diagram (about 290 miles per hour for the test airplane) and with the center of gravity located at the stick-fixed neutral point. For this report, however, the maximum maneuvering tail load was calculated for an altitude of 15,000 feet and for the test center-of-gravity position of 30.3 percent of the mean aerodynamic chord. This was done to provide a consistent basis for comparison with the experimental results. From reference 4 it was found that these deviations from the specifications result in less than a 10-percent decrease in the maximum computed maneuvering tail load. Assuming an elevator motion (fig. 26), the maximum tail-load increment from zero load factor was determined by the method of reference 5. An increment of tail load of 5120 pounds was obtained corresponding to a change in load (acceleration) factor of 7.25. Since the calculated balancing tail load at 290 miles per hour is −362 pounds (reference 1), the limit tail load for the condition investigated is

4758 pounds, and the limit asymmetric tail load is 2379 pounds $\left(\frac{4758}{2}\right)$. The limit root bending moment of 6840 foot-pounds and torsional moment of 6840 pound-feet were obtained by multiplying one-half the maximum load by the calculated lateral distance to the center of pressure of 2.875 feet.

The limit values of asymmetric load, root bending moment, and fuselage torsional moment are compared with experimental values for several conditions in table II. These conditions were chosen to bracket the maximum possible asymmetric loading obtainable in flight for the test airplane. The procedure used to evaluate the experimental values of asymmetric load, root bending moment and fuselage torsional moment for comparison with the limit values is outlined in the appendix. It should be noted again that the validity of the values of asymmetric load and torsional moment speeds higher than 290 miles per hour depends on the assumption that there is no change in slope of the $C_{N_{t_A}}$ versus β and C_{M_T} versus β curves with Mach number.

Although the table shows that the limit asymmetric load and fuselage torsional moment are conservative as compared with the maximum experimental values, the design root bending moment underestimates the actual value on the left tail by almost 25 percent as the calculated center of pressure is inboard of the actual value, and the limit load is less than the experimental load on the left tail.

CONCLUSIONS

From an analysis of the horizontal tail loading obtained in several conditions of flight on a tractor-propeller-driven pursuit airplane and from a comparison of the experimental results with limit values computed on the basis of current Army specifications, several conclusions may be drawn. Although based on results obtained on a specific test airplane, these conclusions which follow are believed to be qualitatively applicable to airplanes of the same general configuration as the test airplane.

1. The changes in horizontal tail loading due to sideslip arise from a large decrease in load and bending moment on the blanketed tail and a small increase of load and bending moment on the leading tail. These changes are relatively independent of power and lift coefficient at speeds of about 290 miles per hour.

2. The asymmetric loads and torsional moments at low speeds and zero angle of sideslip are unimportant even with power on.

3. For large angles of sideslip at high speeds, the total fuselage torsion may become critical since the torsional moment due to asymmetric tail loads is in the same direction as that resulting from vertical-tail loads.

4. Critical bending moments may occur on the left tail in left sideslip at moderate speeds and at the limit load factor (upper left-hand corner of the V-g diagram) if the limit up-load on the left tail does not include the increments in load due to both the asymmetric load existing at zero sideslip and that due to an increase in sideslip angle. (For the test airplane, the lateral center of pressure remained practically constant on the leading tail and moved inboard on the trailing tail with an increase in sideslip angle.)

5. Critical balancing down-loads on the tail may occur at high speeds in sideslipping unaccelerated flight because the increments of negative total tail load with sideslip angle add to the initially high down-loads required to balance the airplane at zero sideslip.

6. The calculated values of asymmetric tail load and fuselage torsional moment due to asymmetric tail loading are conservative as compared with the experimental values for critical flight conditions.

7. The calculated root bending moment may be unconservative by as much as 25 percent as compared with the actual value for critical flight conditions.

Ames Aeronautical Laboratory,
National Advisory Committee for Aeronautics,
Moffett Field, Calif., October 1946.

APPENDIX

Evaluation of Flight Loads for Various Conditions

Asymmetric loads.- The asymmetric loads in steady unaccelerated flight for values of C_L of 0.171 and 0.069 were taken directly from figure 17 of this report. In order to determine the asymmetric load for $C_L = 1.25$ $(V_i = 290 \text{ mph})$ and $\beta = -10^\circ$ in accelerated flight $(A_Z = 7.33)$, it was necessary to use the $C_{N_{t_A}}$ versus β curve for a C_L of 0.80 in figure 14 since no data were obtained at much higher values of C_L. The use of this curve was justified as the available data showed relatively small changes of $C_{N_{t_A}}$ with C_L. The difference in N_{t_A} of 343 pounds corresponding to a difference in $C_{N_{t_A}}$ of 0.40 between 0° and −10° sideslip was added to the asymmetric load at zero sideslip (435 lb from fig.

29 of reference 1) resulting in an asymmetric load of 778 pounds for the condition considered. In an analogous manner, the asymmetric loads for $C_L = 0.51$ ($V_i = 463$ mph) at $\beta = -5^\circ$ and -10° were obtained by adding the difference in N_{t_A} corresponding to a difference in $C_{N_{t_A}}$ between 0° and -5°, and 0° and -10°, respectively, for an interpolated C_L of 0.51 in figure 14 to the asymmetric load at zero sideslip obtained from figure 29 of reference 1. There is obtained

$$N_{t_A}\begin{pmatrix} C_L = 0.51 \\ \beta = -5^\circ \end{pmatrix} = 545 + 840 = 1385 \text{ pounds}$$

and

$$N_{t_A}\begin{pmatrix} C_L = 0.51 \\ \beta = -10^\circ \end{pmatrix} = 1075 + 840 = 1915 \text{ pounds}$$

Root bending moment.- The root bending moment in steady unaccelerated flight at 290 miles per hour and -10° sideslip was determined from the value of $C_{M_{r_L}}$ given in the power-on curve for $C_L = 0.2$ in figure 18. The first step in obtaining the bending moment for $C_L = 1.25$ ($V_i = 290$ mph; $A_Z = 7.33$) and $\beta = -10^\circ$ was to determine the left-tail load corresponding to these conditions. (The left tail is used since it experiences the higher load in left sideslip.) The calculated load of 4758 pounds was assumed for the experimental total tail load at zero sideslip, since experimental data for similar conditions were not available. The asymmetric load of 435 pounds obtained from figure 29 of reference 1 was apportioned symmetrically over each side of the tail; that is, the left-tail load was increased by 218 pounds and the right-tail load reduced by a like amount. Applying this dissymmetry to the 4758 pounds, there is obtained a load of $\frac{4758}{2} + 218 = 2597$ pounds on the left tail at zero sideslip. From the power-on $C_{N_{t_L}}$ versus β curve for $C_L = 0.80$ (assuming, as before, unimportant changes from $C_L = 0.80$ to $C_L = 1.25$) in figure 10, an increase in $C_{N_{t_L}}$ of 0.013 from 0° to -10° sideslip was obtained corresponding to an increase in left-tail load of 111 pounds. Therefore, the left-tail load for the condition investigated is 2597 + 111 = 2708 pounds. Multiplying this value by the lateral center of pressure at $\beta = -10^\circ$ (3.24 ft from fig. 20) gives a root bending moment of 8770 foot-pounds.

Torsional moments.– The torsional moments in steady unaccelerated flight for values of C_L of 0.171 and 0.069 were obtained directly from figure 25. In a manner similar to that used for determining the asymmetric loads, the fuselage torsional moments for $C_L = 1.25$ (V_i = 290 mph; A_Z = 7.33) were derived from figure 21 of this report and figure 30 of reference 1.

REFERENCES

1. Sadoff, Melvin, Turner, William N., and Clousing, Lawrence A.: Measurements of the Pressure Distribution on the Horizontal-Tail Surface of a Typical Propeller-Driven Pursuit Airplane in Flight. I – Effects of Compressibility in Steady Straight and Accelerated Flight. Proposed TN. (Originally NACA CMR No. A5H28, 1945)

2. Clousing, Lawrence A., Turner, William N., and Rolls, L. Stuart: Measurements in Flight of the Pressure Distribution on the Right Wing of a P-39N-1 Airplane at Several Values of Mach Number. NACA ARR No. 4K09, 1945.

3. Sweberg, Harold H., and Dingeldein, Richard C.: Effects of Propeller Operation and Angle of Yaw on the Distribution of the Load on the Horizontal Tail Surface of a Typical Pursuit Airplane. NACA ARR No. 4B10, 1944.

4. Kelley, Joseph, Jr., and Missall, John W.: Maneuvering Horizontal Tail Loads. AAF TR No. 5185, 1945.

5. Pearson, Henry A.: Derivation of Charts for Determining the Horizontal Tail Load Variation with Any Elevator Motion. NACA ARR, Jan., 1943.

TABLE I.- ORDINATES AT PRESSURE ORIFICES ON HORIZONTAL TAIL OF THE TEST AIRPLANE

[All values are in percent of chord]

Orifice	Row A				Row B				Row C				Row D			
	Upper surface		Lower surface		Upper surface		Lower surface		Upper surface		Lower surface		Upper surface		Lower surface	
	Station	Ordinate	Station	Ordinate	Station	Ordinate	Station	Ordinate	Station	Ordinate	Station	Ordinate	Station	Ordinate	Station	Ordinate
Left side																
1	1.44	1.55	1.55	1.55	2.57	1.70	2.84	1.70	1.61	1.24	1.24	1.14	2.08	1.40	2.21	1.43
2	10.15	3.51	9.37	3.51	10.43	3.23	9.88	3.27	7.30	2.43	7.08	2.48	25.04	3.15	24.98	3.09
3	30.96	4.48	30.96	4.64	31.89	4.11	31.95	4.21	20.35	3.28	20.25	3.38	46.14	2.93	46.34	2.93
4	47.10	4.13	46.44	4.23	42.61	2.95	42.66	3.91	31.06	3.35	33.79	3.45	57.56	2.11	57.72	2.11
5	57.48	3.80	57.28	3.72	54.55	3.55	54.65	3.52	46.91	3.03	46.71	3.01	70.60	1.95	70.99	1.95
6	62.54	1.80	62.54	1.86	59.77	1.52	59.88	1.86	57.29	2.19	57.44	2.36	79.80	1.40	80.00	1.37
7	68.98	2.79	69.04	2.89	68.93	2.61	68.98	2.84	67.58	2.09	68.05	1.99	-----	----	-----	----
8	82.64	1.65	82.68	1.75	80.68	1.66	80.84	1.73	83.73	1.17	83.73	.99	-----	----	-----	----
Right side																
1	1.34	1.45	1.51	1.45	2.02	1.59	2.40	1.70	1.96	1.49	2.43	1.49	1.98	1.50	2.02	1.24
2	10.10	3.57	10.03	3.45	10.06	3.27	10.43	3.29	9.80	3.00	10.12	2.75	25.24	3.24	26.18	3.09
3	30.90	4.55	30.86	4.47	31.75	4.20	31.86	4.08	35.56	3.66	36.08	3.29	45.37	2.93	45.85	3.06
4	47.70	4.10	47.22	4.16	43.08	3.92	43.08	3.83	49.02	3.29	49.28	3.14	58.86	2.44	58.37	1.95
5	57.70	3.70	57.54	3.74	54.33	3.63	54.42	3.51	60.13	2.75	60.42	2.14	71.54	2.11	70.93	1.95
6	63.33	2.17	62.40	1.86	59.36	1.95	59.52	1.59	71.11	2.17	71.24	1.91	80.16	1.63	80.03	1.37
7	68.67	2.77	68.60	2.92	68.89	2.74	69.14	2.72	84.97	1.20	84.97	1.18	-----	----	-----	----
8	82.25	1.80	82.11	2.05	78.23	2.02	78.28	1.97	-----	----	-----	----	-----	----	-----	----
9	-----	----	-----	----	86.96	1.36	86.73	1.36	-----	----	-----	----	-----	----	-----	----

NATIONAL ADVISORY
COMMITTEE FOR AERONAUTICS

TABLE II.- COMPARISON OF LIMIT VALUES OF ASYMMETRIC LOAD, ROOT BENDING MOMENT AND FUSELAGE TORSIONAL MOMENT WITH EXPERIMENTAL VALUES[a]

EXPERIMENTAL VALUES[a]									
Item	Limit Value	Source	Steady unaccelerated flight (A_Z = 1.0)			Accelerated flight (A_Z = 7.33)			Source
			C_L = 0.171 V_1 = 290 mph β = -10°	C_L = 0.069[b] V_1 = 463 mph β = -5°	C_L = 0.069[b] V_1 = 463 mph β = -10°	C_L = 1.25[b] V_1 = 290 mph β = -10°	C_L = 0.51[b] V_1 = 463 mph β = -5°	C_L = 0.51[b] V_1 = 463 mph β = -10°	
Asymmetric load	2379 lb	Half of load calculated by method of ref. 6.	550 lb	1070 lb	1725 lb	778 lb	1385 lb	1915 lb	See appendix
Root bending moment	6840 ft-lb	Half of maximum load x calculated center of pressure	874 ft-lb	(c)	(c)	8770 ft-lb	(c)	(c)	See appendix
Fuselage torsional moment	6840 lb-ft	Half of maximum load x calculated center of pressure	2100 lb-ft	3800 lb-ft	6700 lb-ft	3030 lb-ft	1200 lb-ft	3680 lb-ft	See appendix

[a] Only power-on data were used to determine the experimental values.

[b] Values estimated from experimental results. Superscript applies to entire column.

[c] These values were not ascertainable because the center-of-pressure distances for these conditions were not available. The bending moments corresponding to these conditions, however would not be critical.

NATIONAL ADVISORY
COMMITTEE FOR AERONAUTICS

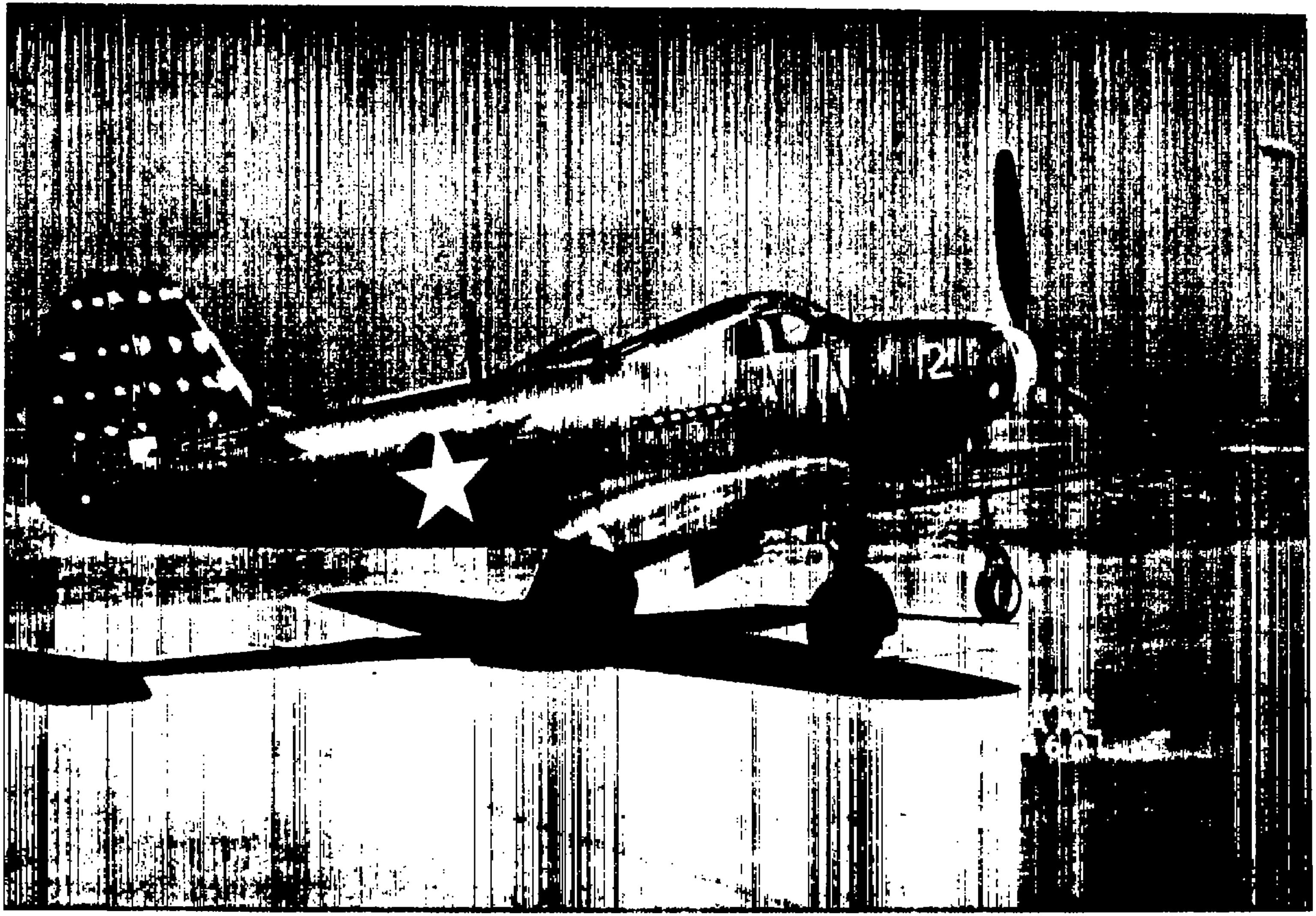

Figure 1.- Three-quarter rear view of test airplane.

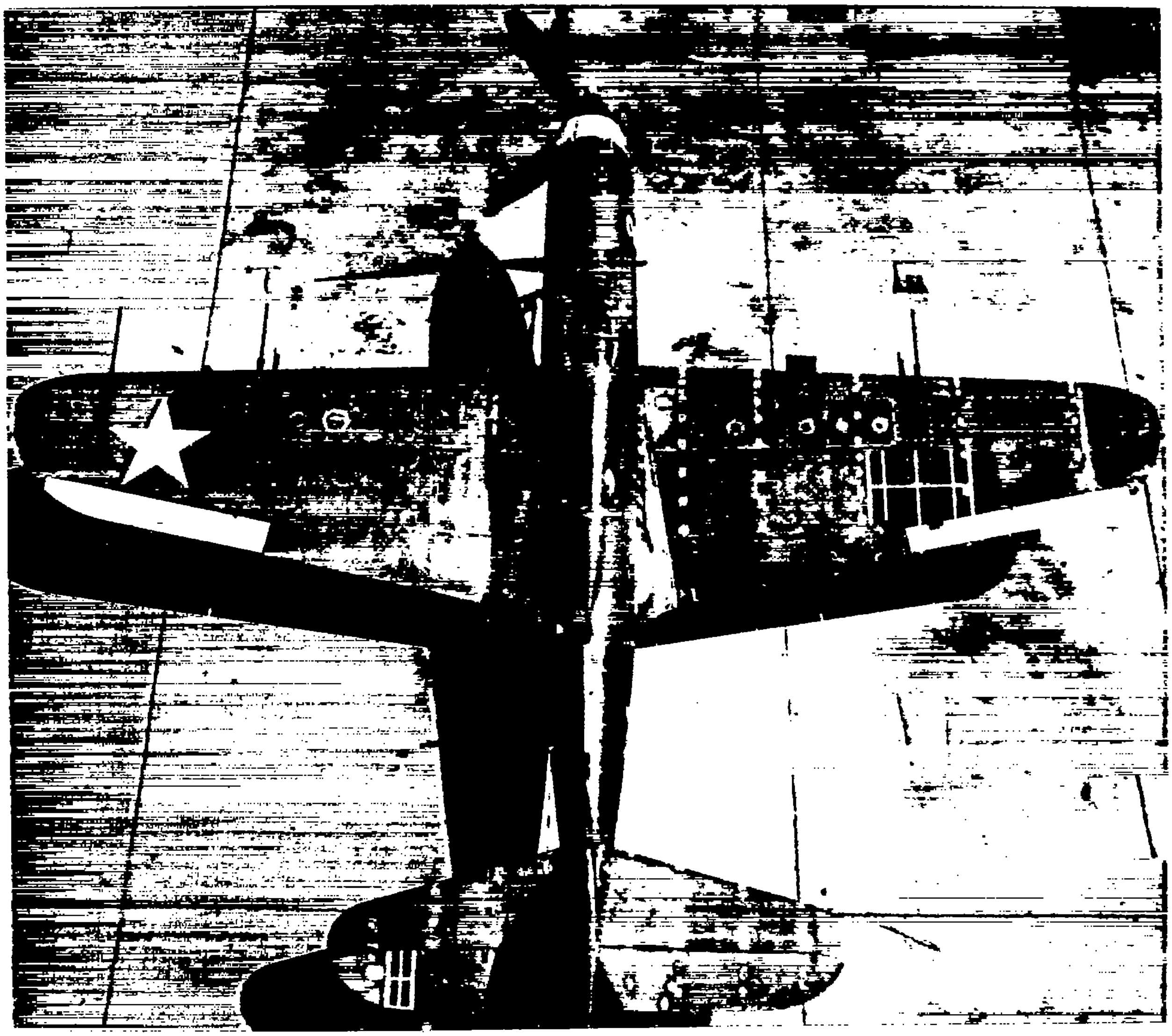

Figure 2.- Top view of test airplane as instrumented for flight tests.

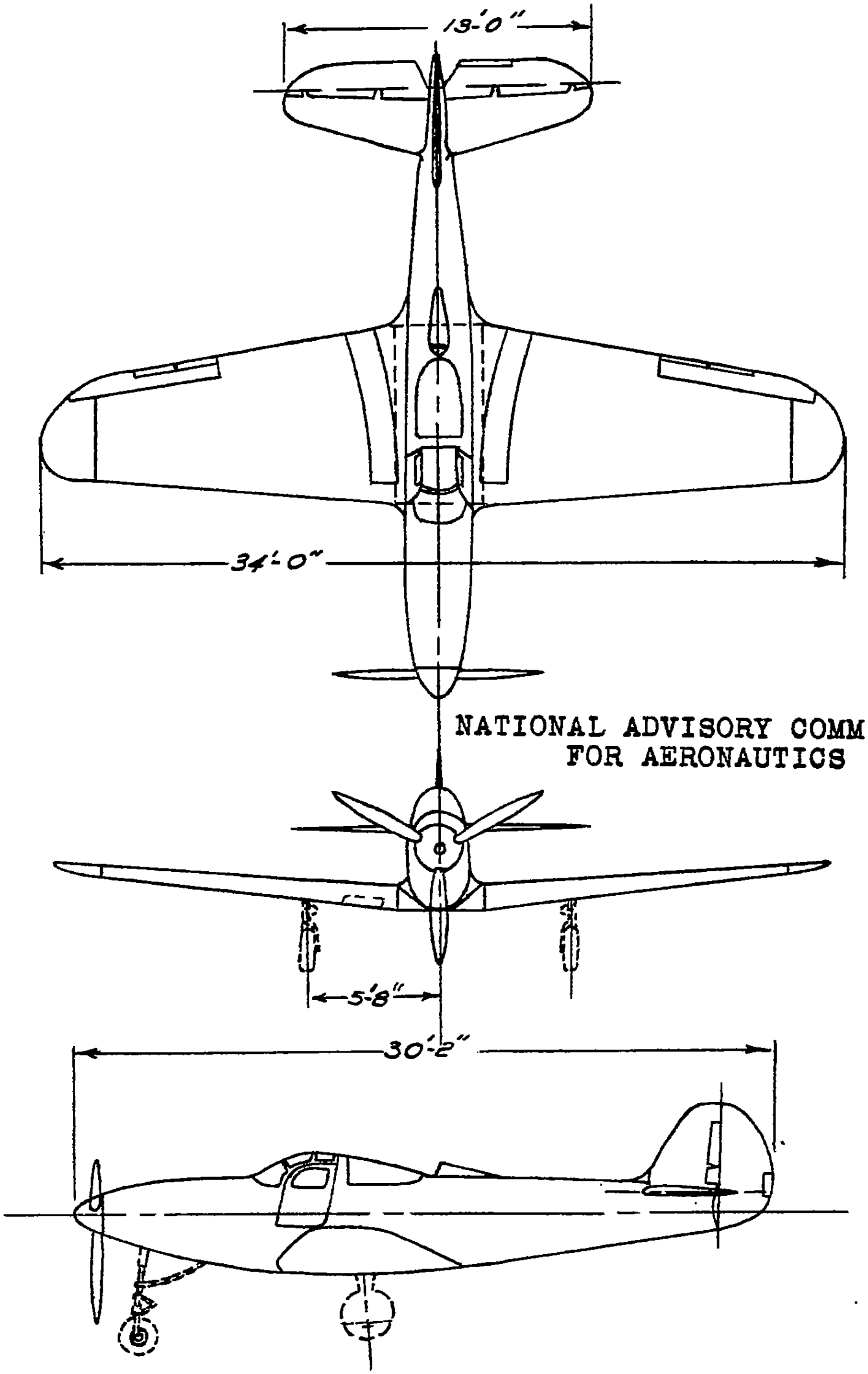
13'-0"
34'-0"
NATIONAL ADVISORY COMMITTEE
FOR AERONAUTICS
5'-8"
30'-2"

Figure 3. – Three-view drawing of the test airplane.

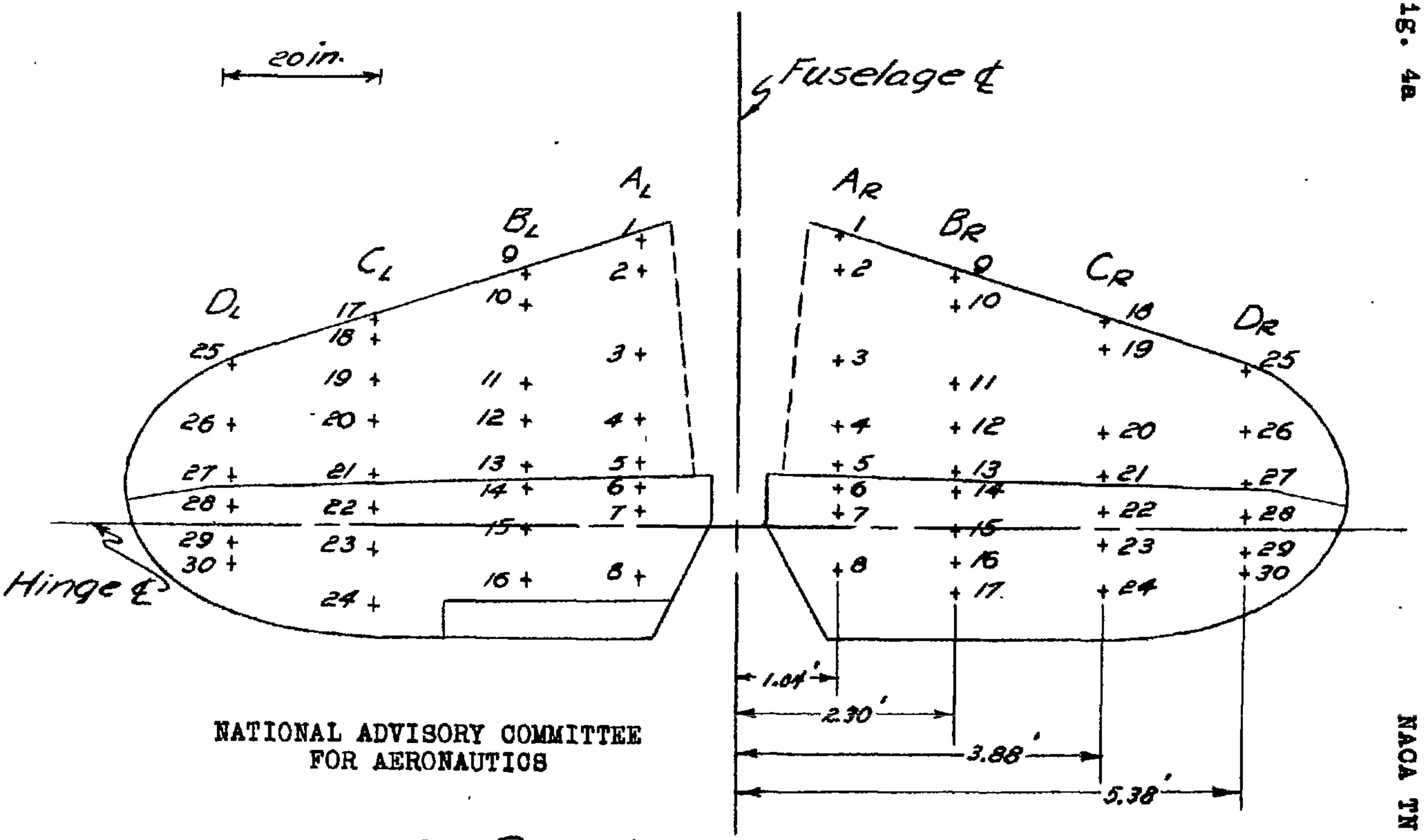
20 in.
Fuselage ℄
A_L
B_L
C_L
D_L
A_R
B_R
C_R
D_R
1
2
3
4
5
6
7
8
9
10
11
12
13
14
15
16
17
18
19
20
21
22
23
24
25
26
27
28
29
30
Hinge ℄
1.04'
2.30'
3.88'
5.38'

NATIONAL ADVISORY COMMITTEE
FOR AERONAUTICS

(a) Plan view

Figure 4.- Orifice locations on horizontal tail. Test airplane.

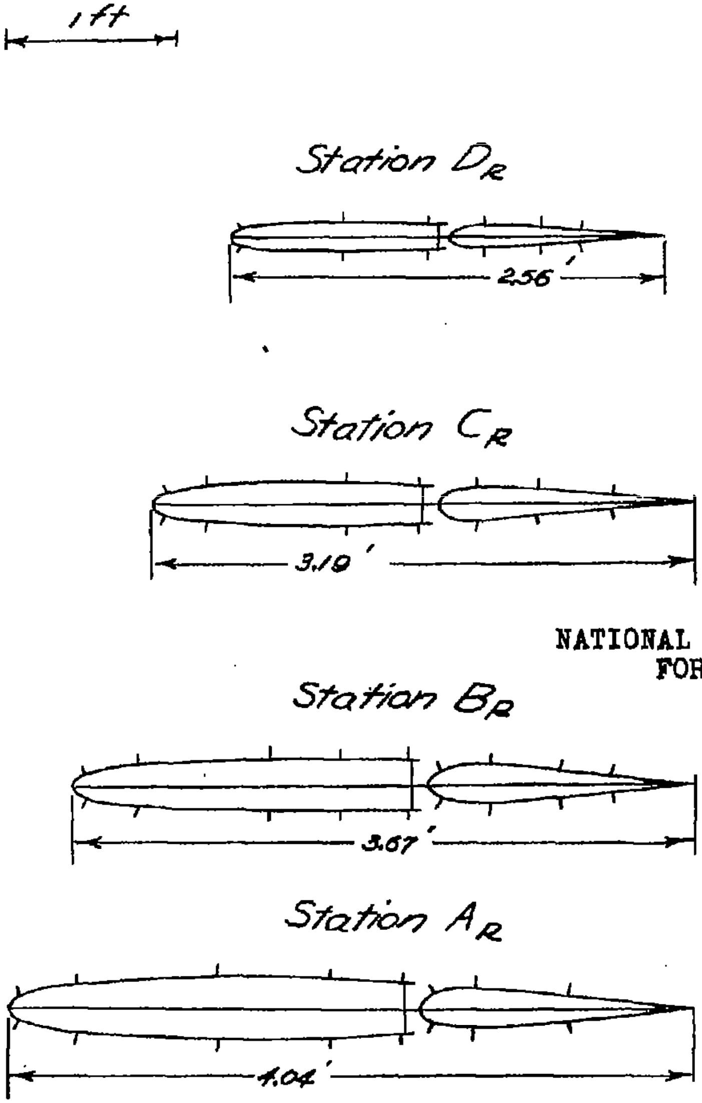
1 ft
Station D_R
2.56'
Station C_R
3.19'
Station B_R
3.67'
Station A_R
4.04'

(b) Right tail sections.

Figure 4. - Continued. Test airplane.

NATIONAL ADVISORY COMMITTEE
FOR AERONAUTICS

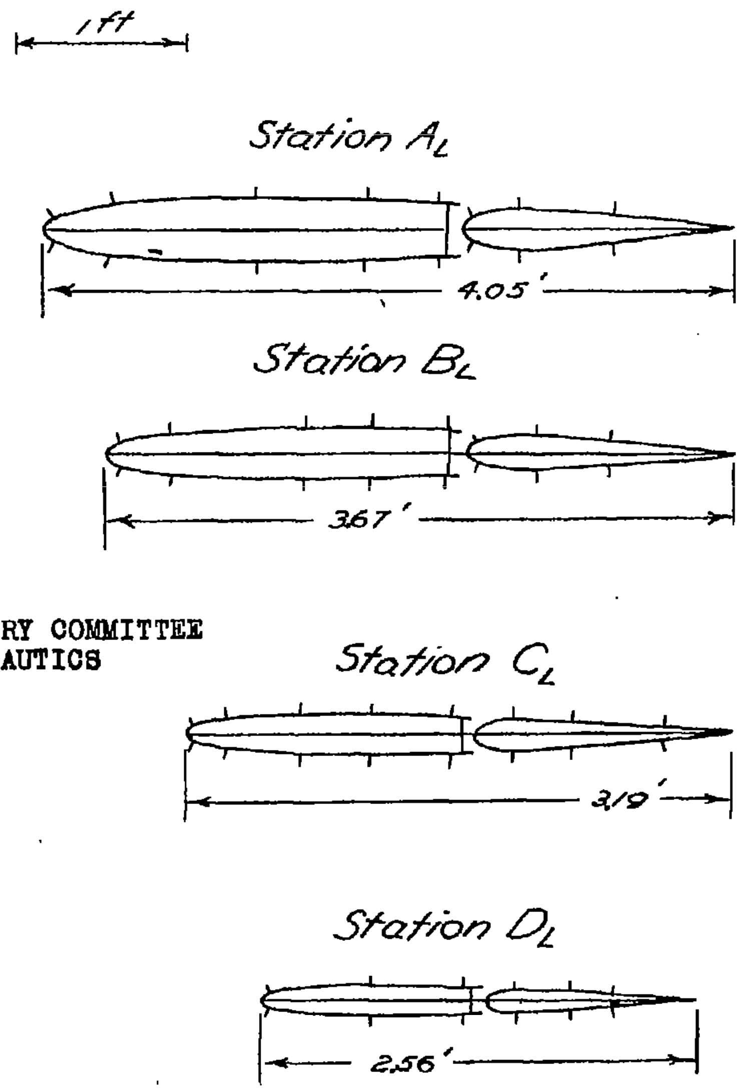
1 ft
Station A_L
4.05'
Station B_L
3.67'
Station C_L
3.19'
Station D_L
2.56'

(c) Left tail sections.

Figure 4. - Concluded. Test airplane.

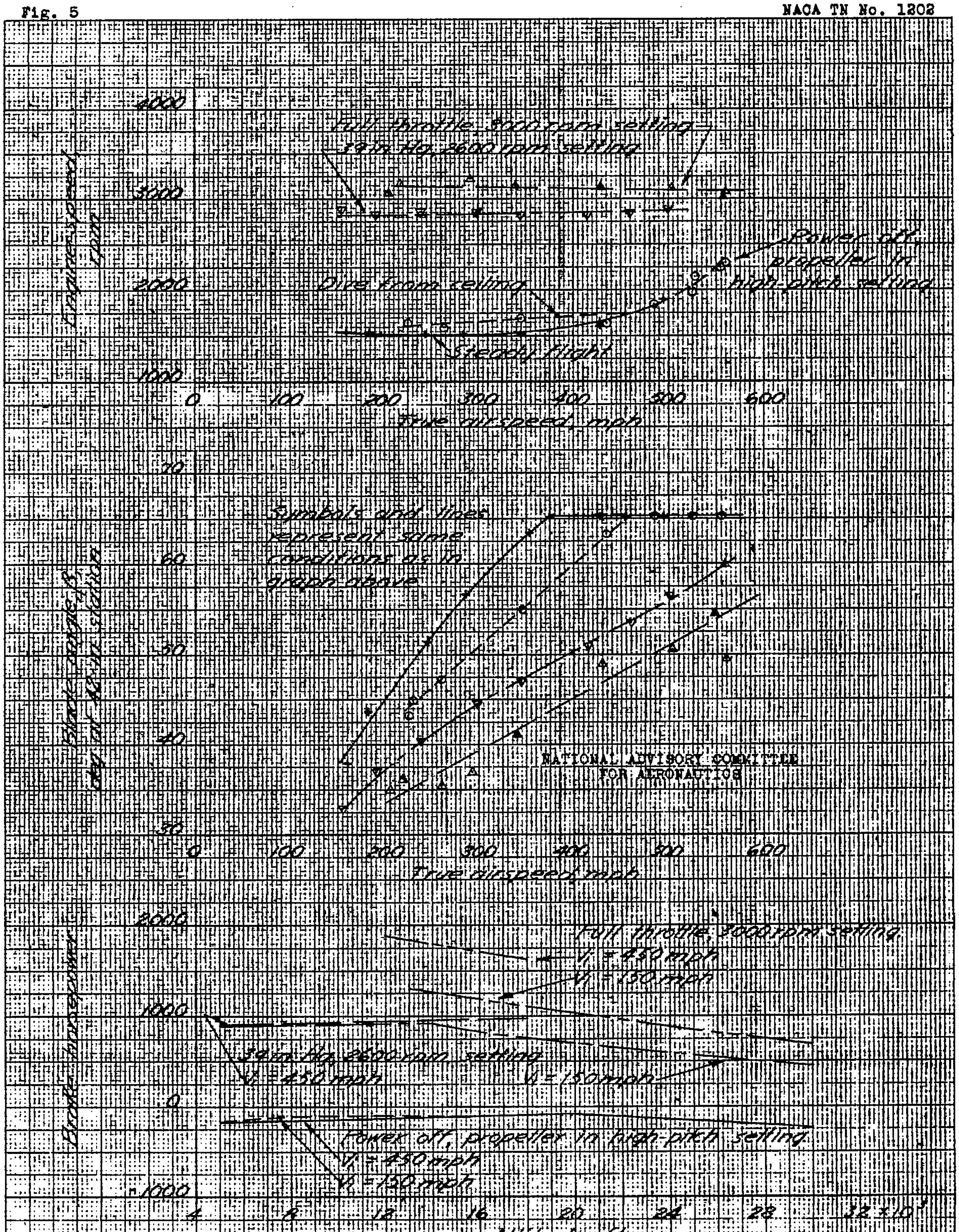

Figure 5.— Engine speed, propeller-blade angle, and brake horsepower obtained for certain power settings.

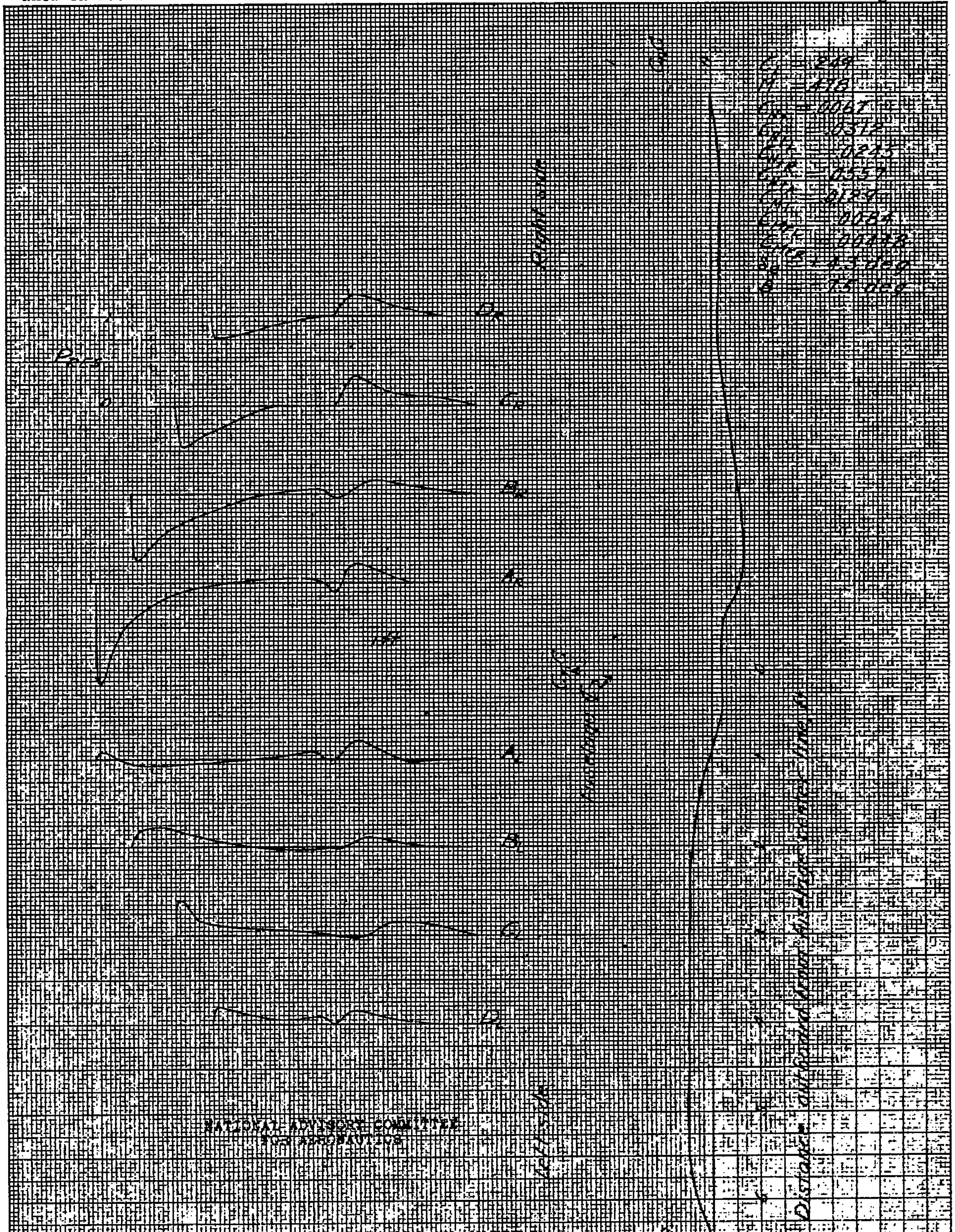

(a) Lift coefficient 0.249; Sideslip angle -7.5°

Figure 6.- Pressure distribution over the horizontal tail in power-on flight.

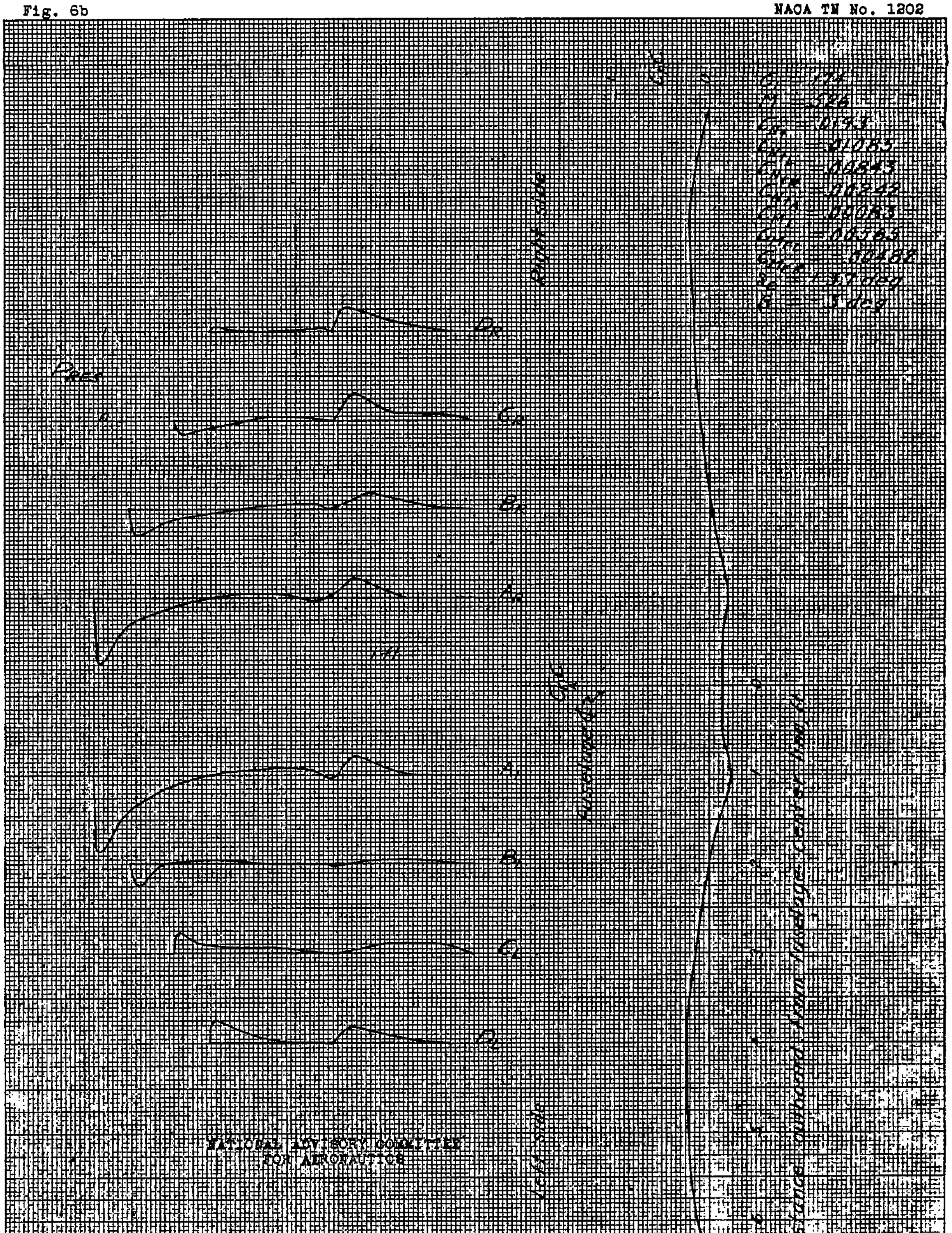

(b) Lift coefficient 0.174, Sideslip angle, -0.5°

Figure 6. – Continued.

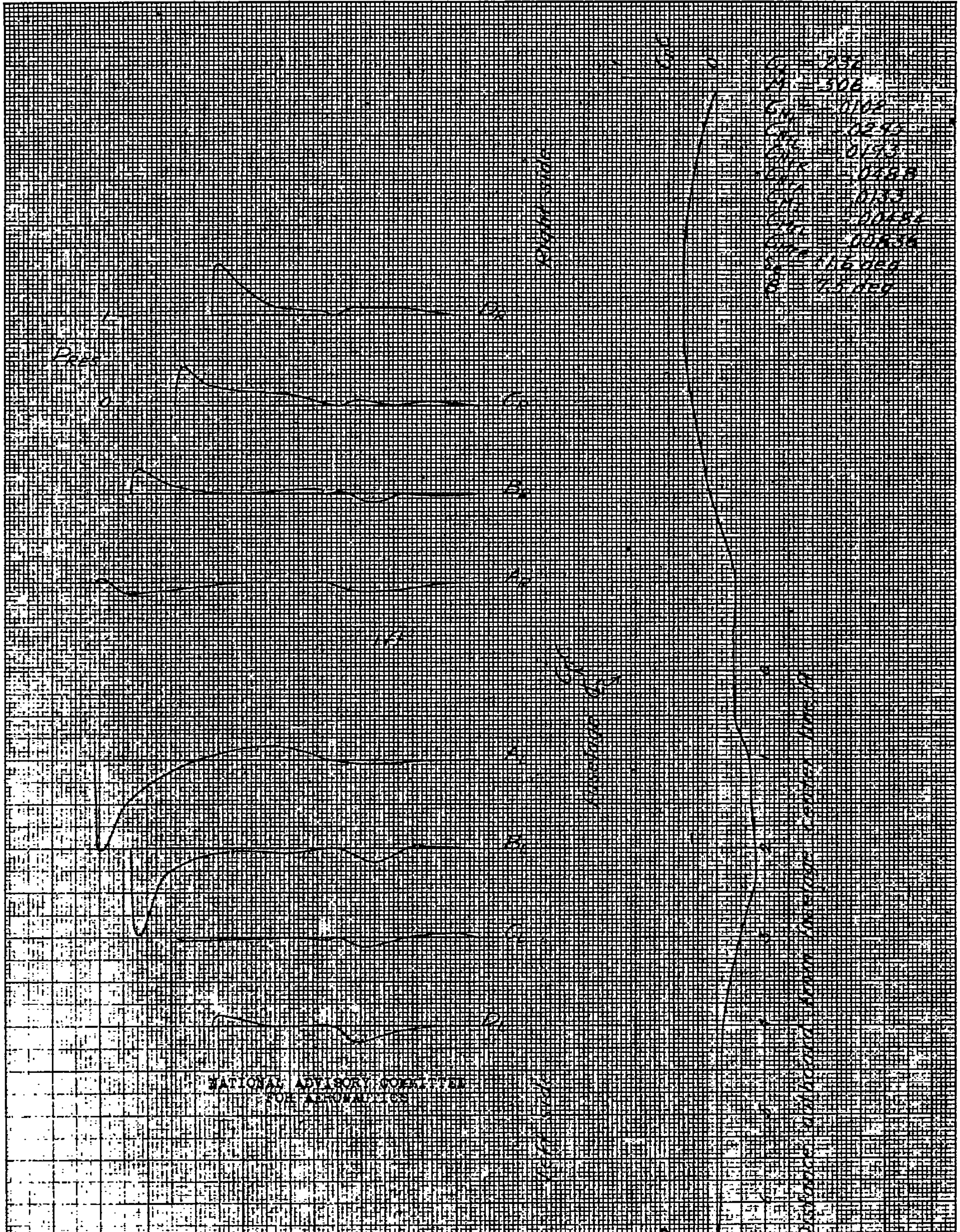

(c) Lift coefficient 0.232; Sideslip angle 7.5°

Figure 6 – Continued.

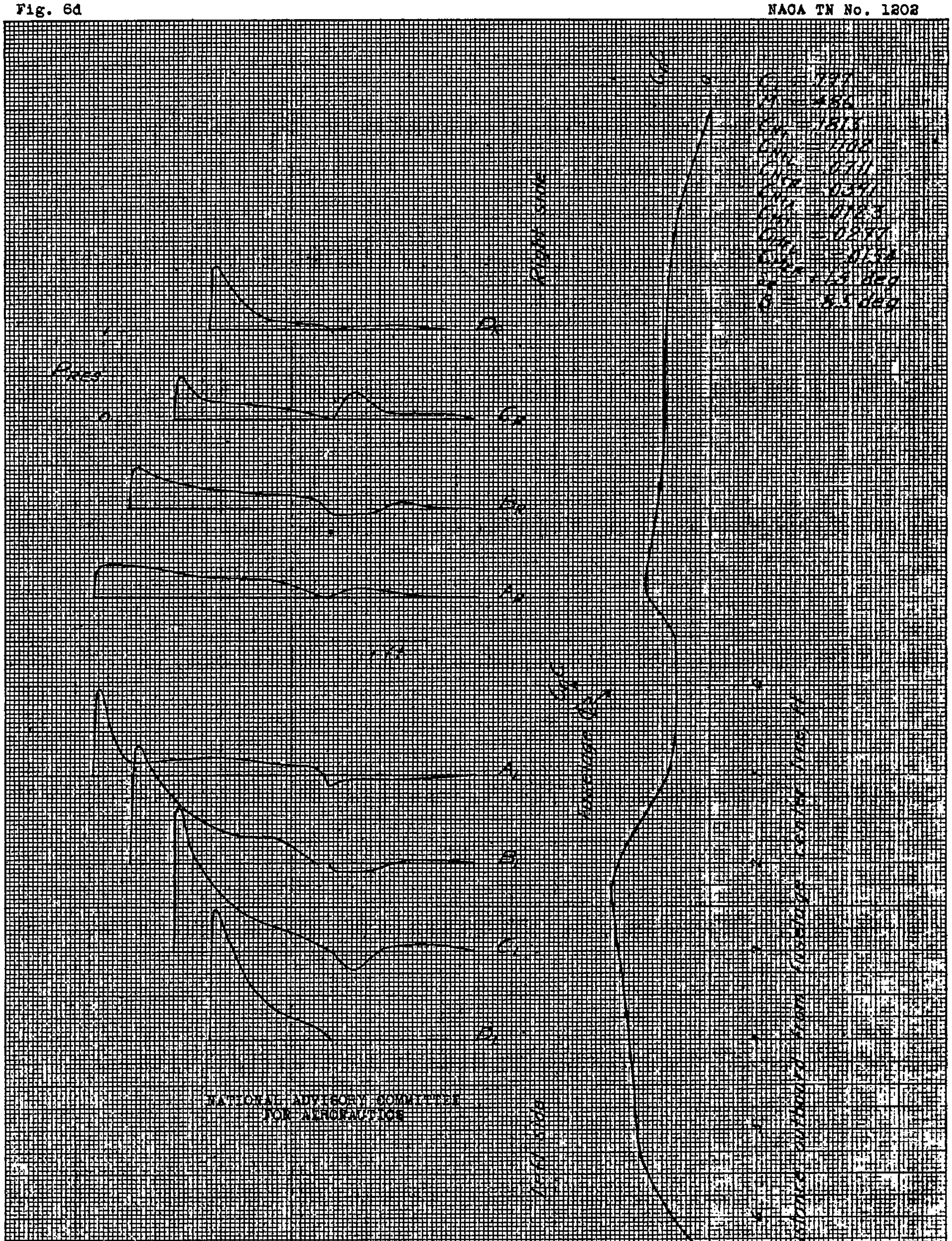

(d) Lift coefficient, 0.797; Sideslip angle, -6.5°

Figure 6. — Continued.

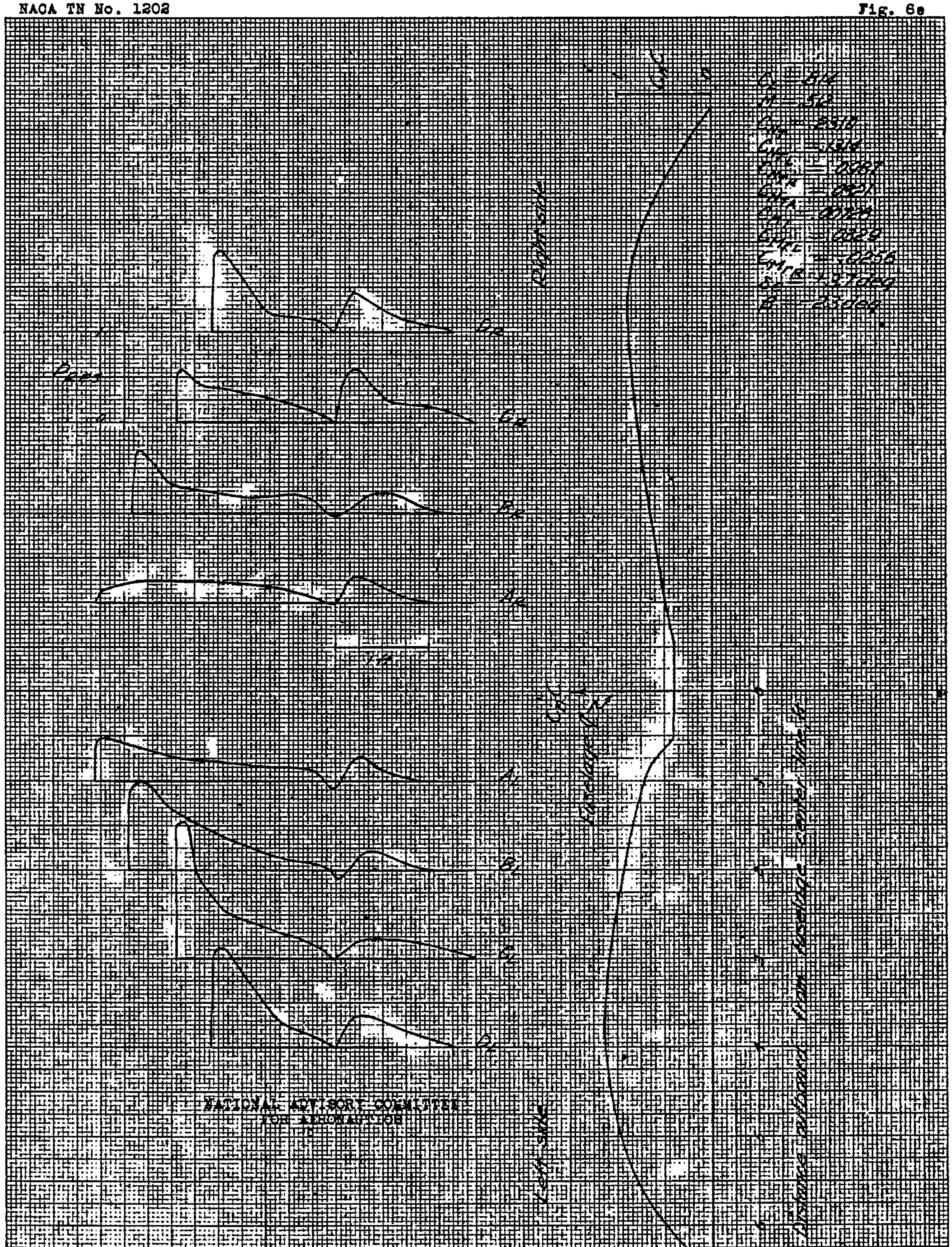

(e) Lift coefficient, 0.814; Sideslip angle, -8.3°

Figure 6.—Continued.

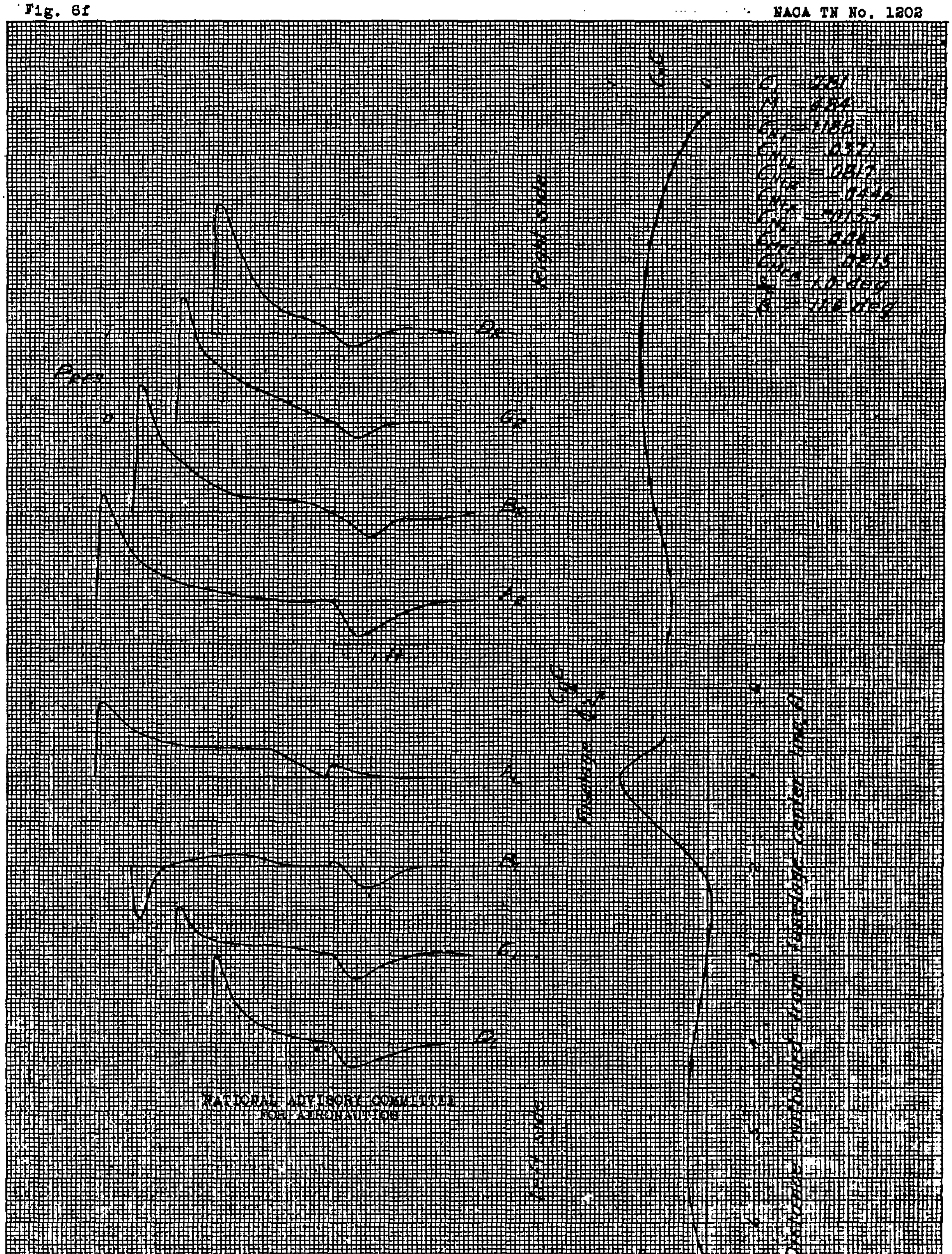

NATIONAL ADVISORY COMMITTEE FOR AERONAUTICS

(f) Lift coefficient, 0.781; Sideslip angle, 11.6°

Figure 6.- Concluded.

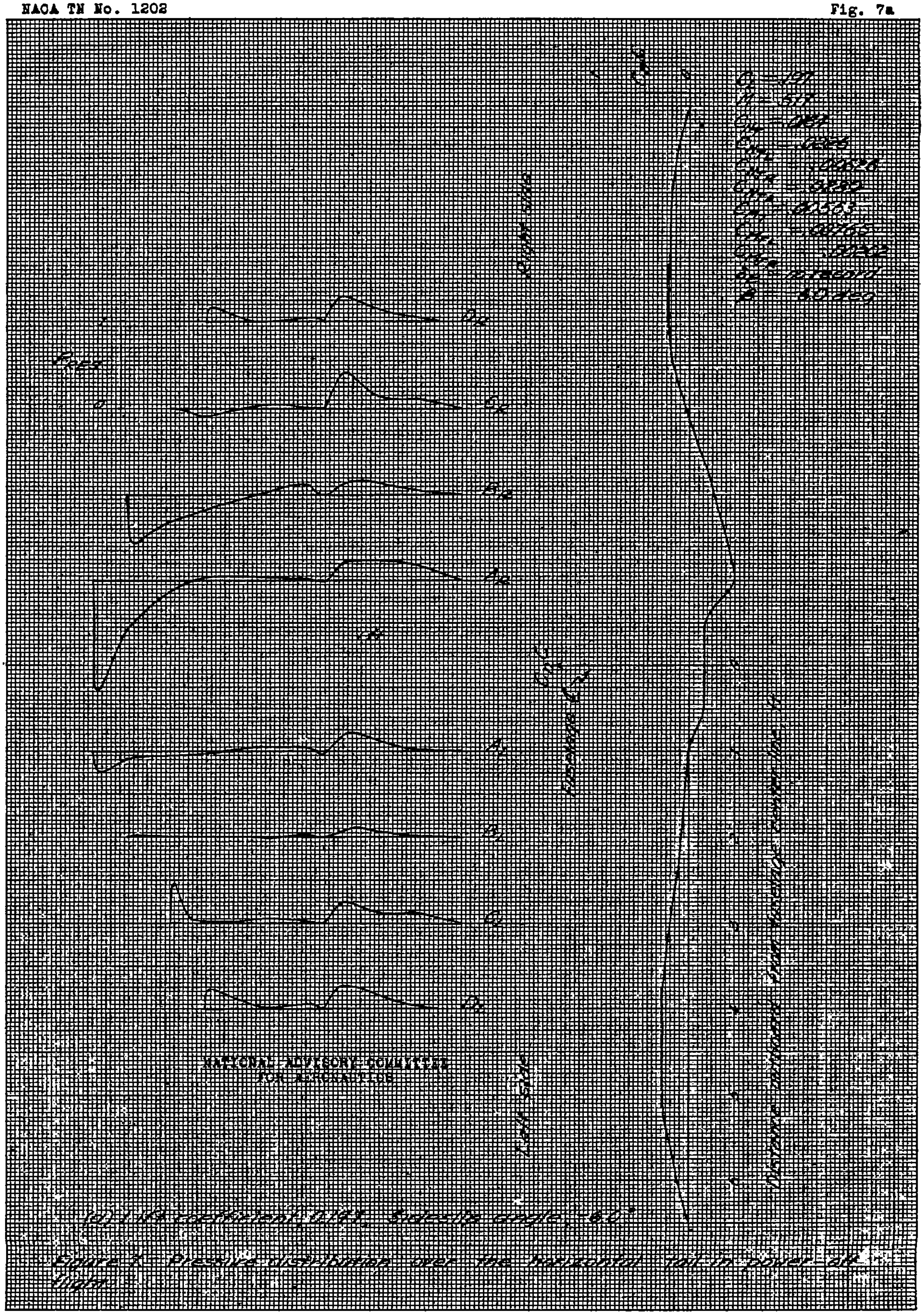

NATIONAL ADVISORY COMMITTEE FOR AERONAUTICS

(a) Lift coefficient, 0.191. Sideslip angle, -6.0°

Figure 7.- Pressure distribution over the horizontal tail in power-off flight.

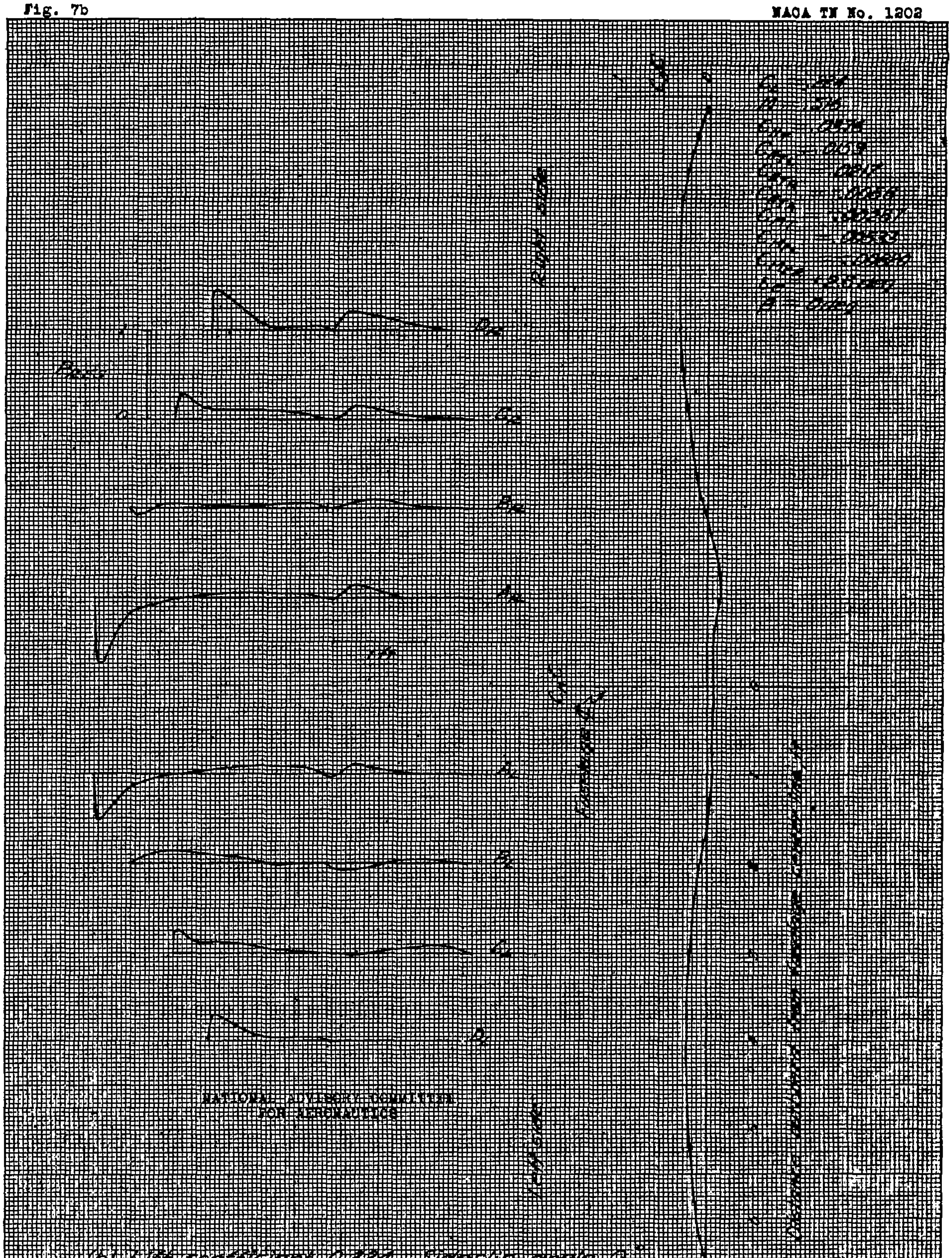

NATIONAL ADVISORY COMMITTEE FOR AERONAUTICS

(b) Lift coefficient, 0.224. Sideslip angle, 0°.

Figure 7.- Continued.

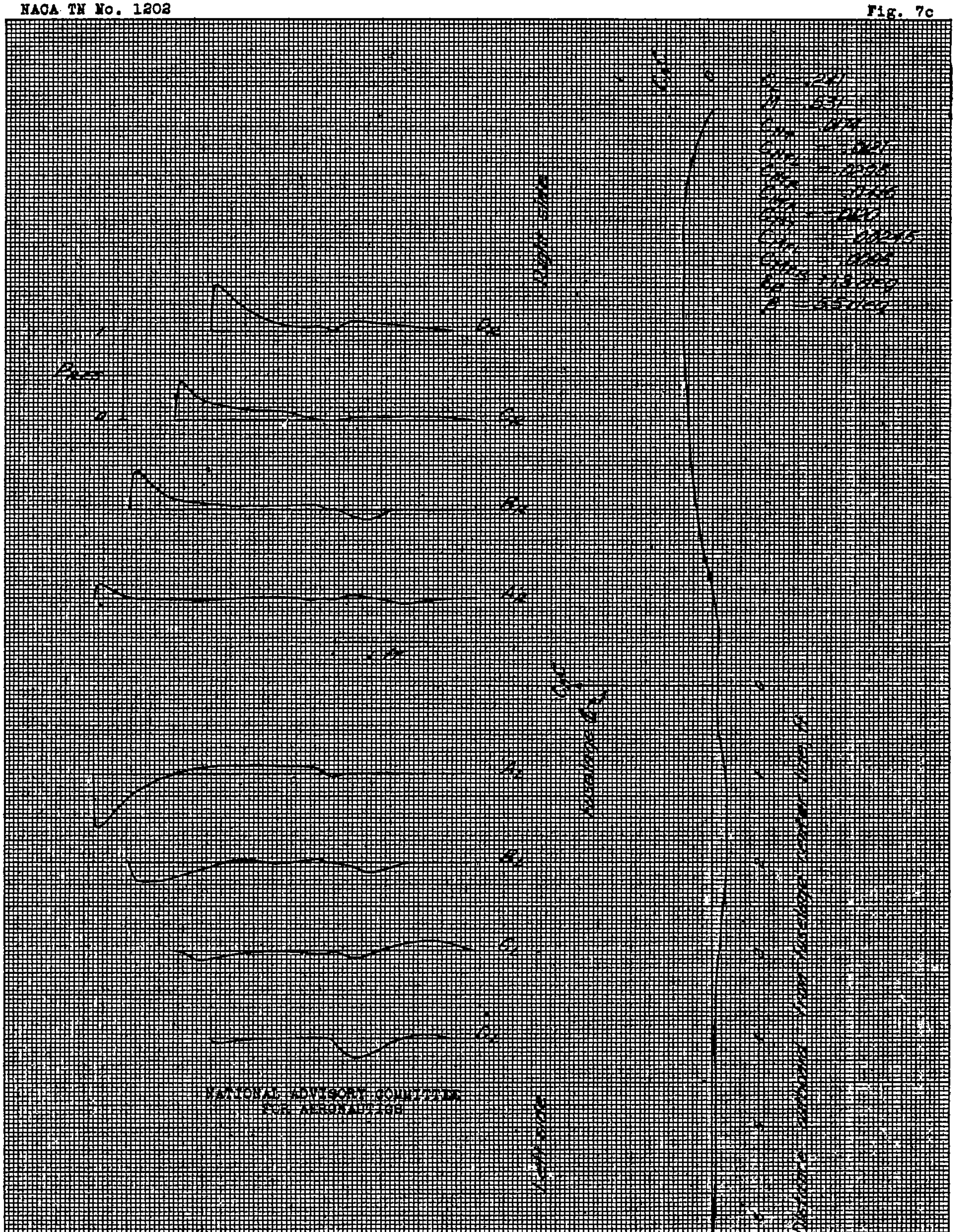

NATIONAL ADVISORY COMMITTEE FOR AERONAUTICS

(c) Lift coefficient, 0.241; Sideslip angle, 5.5°

Figure 7- Continued.

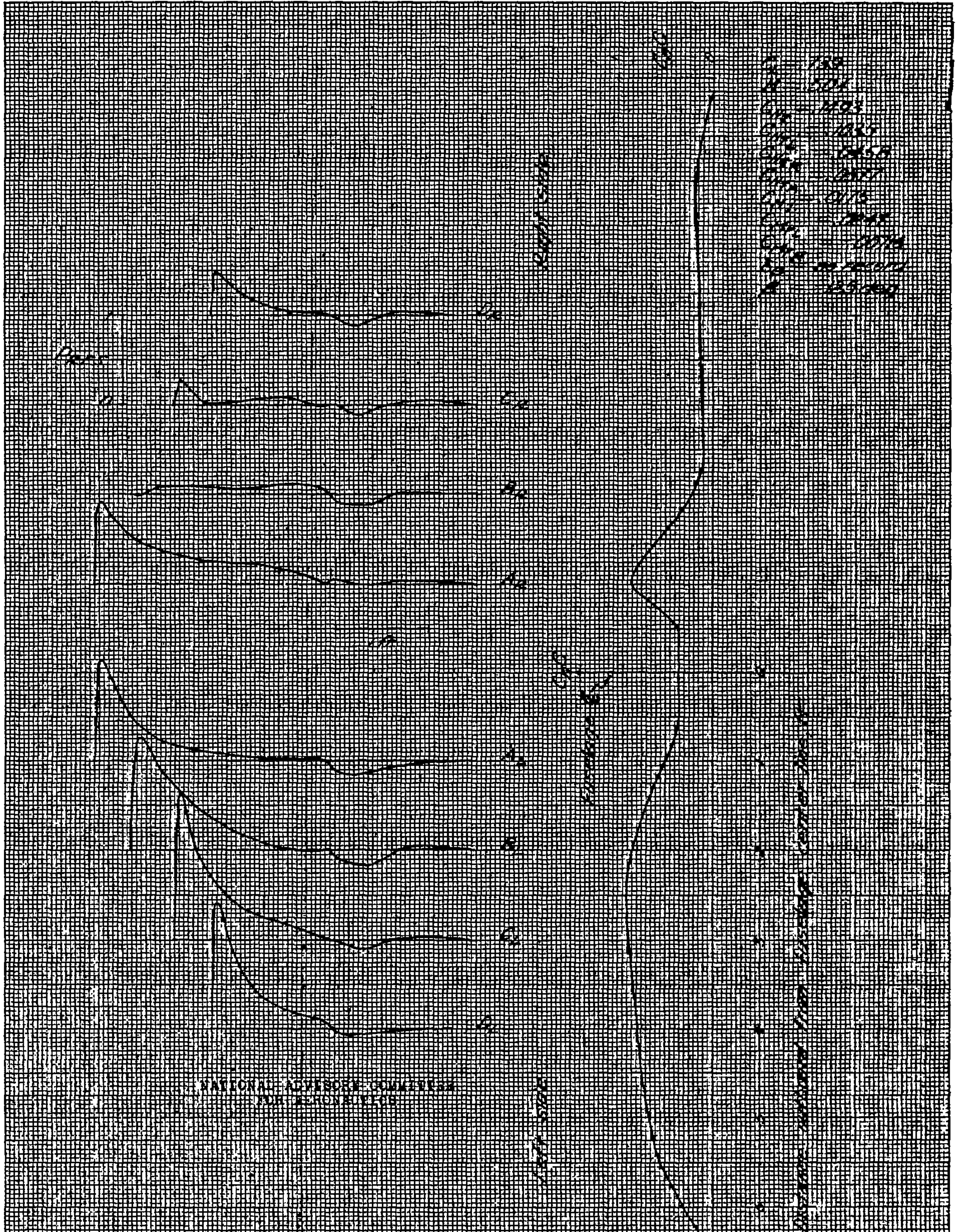

(d) Lift coefficient, 0.352; Sideslip angle, -12.5°

Figure 7 - Continued.

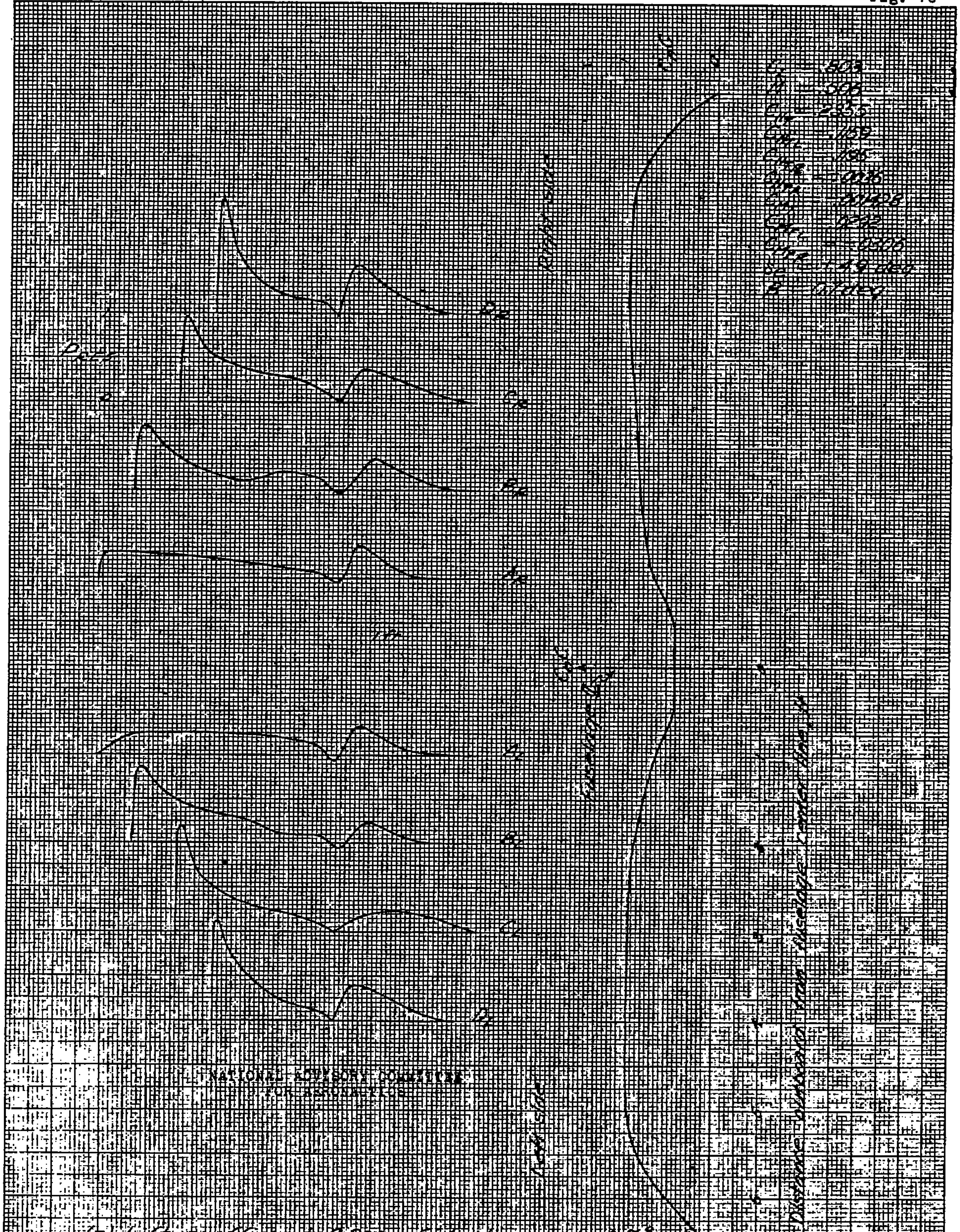

(e) Lift coefficient, 0.503; sideslip angle, 0.7°.

Figure 7.- Continued.

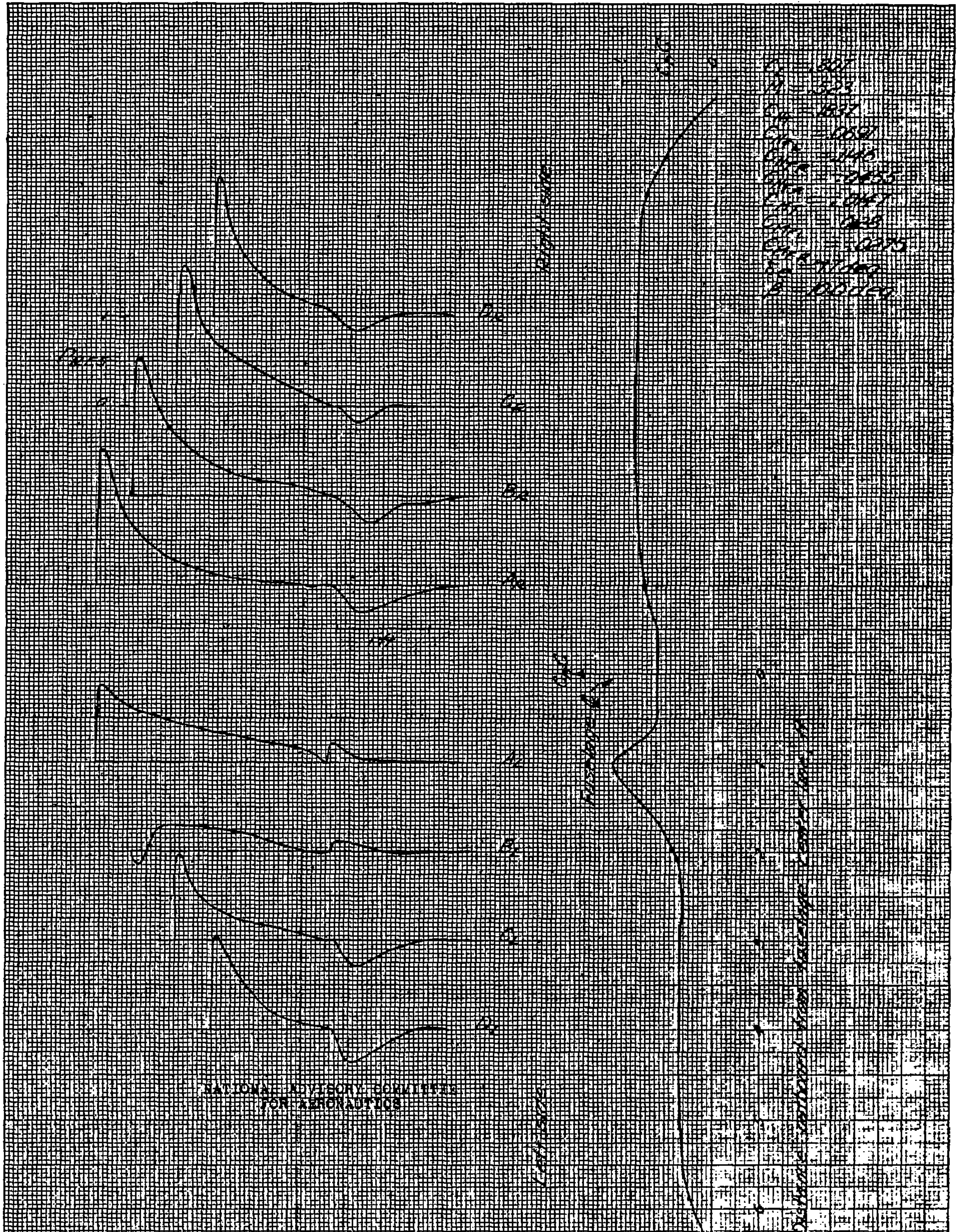

(f) Lift coefficient, 0.602. Sideslip angle, 10.0°.

Figure 7.- Concluded.

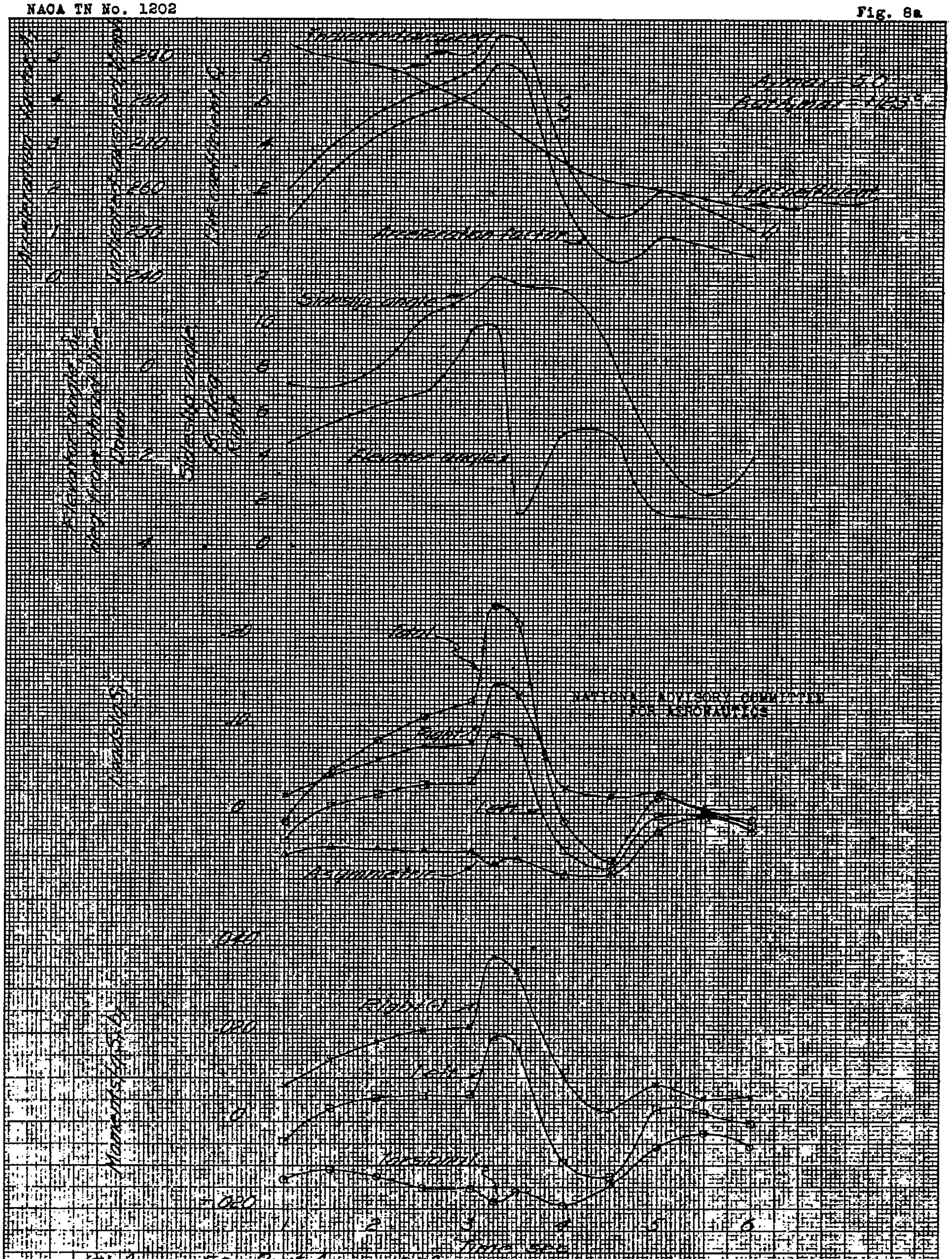

(a) $A_{z_{max}}$, 5.0; β at $A_{z_{max}}$, 12.8°.

Figure 8.- Time histories of power-on sideslipping pull-ups at approximately 290 miles per hour.

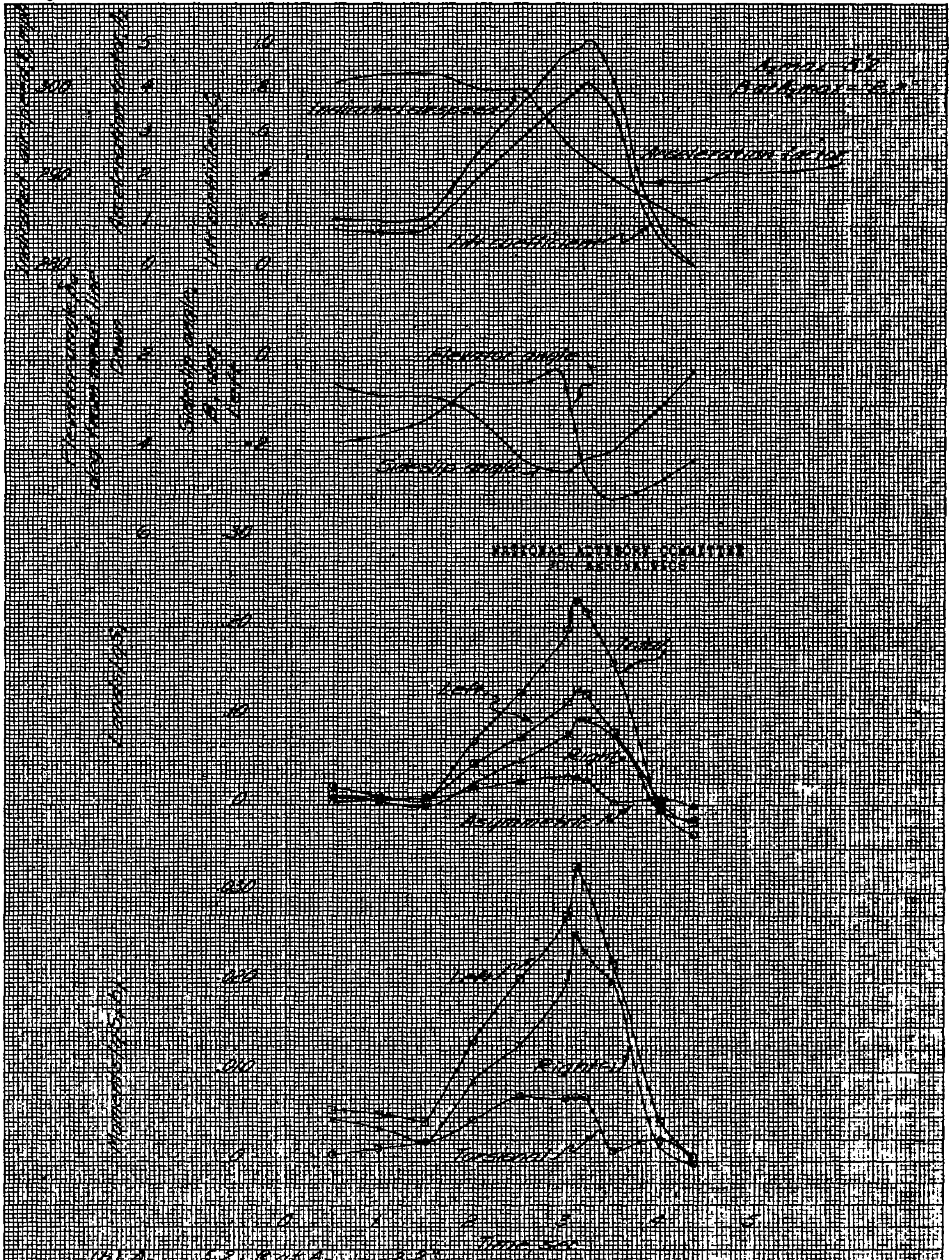

NATIONAL ADVISORY COMMITTEE FOR AERONAUTICS

(b) Δ_{max}, 5.2; R of Δ_{max}, 2.4.

Figure 8.- Continued.

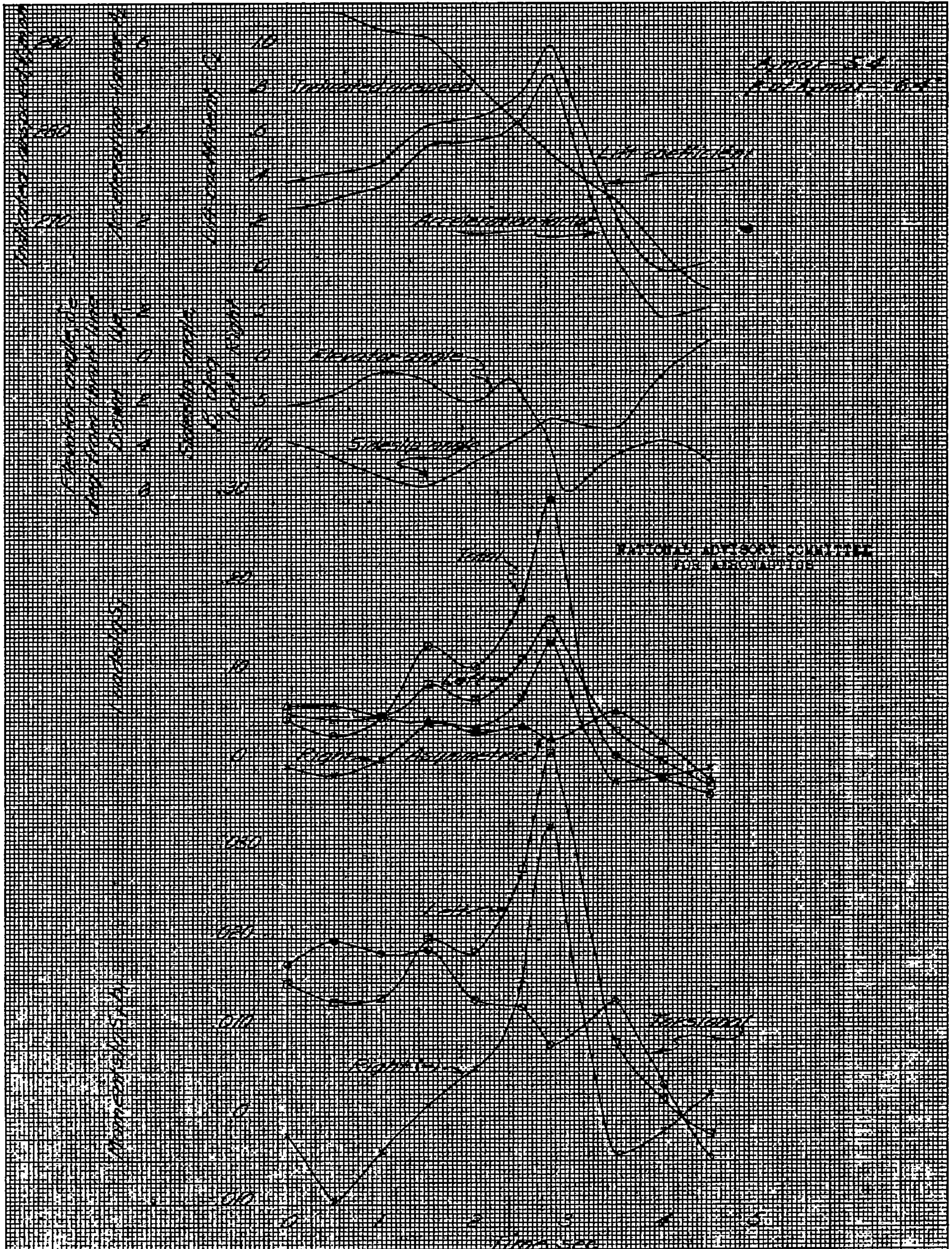

(c) A_{max} 5.4; Tail A_{max} - 6.4

Figure 8. Concluded.

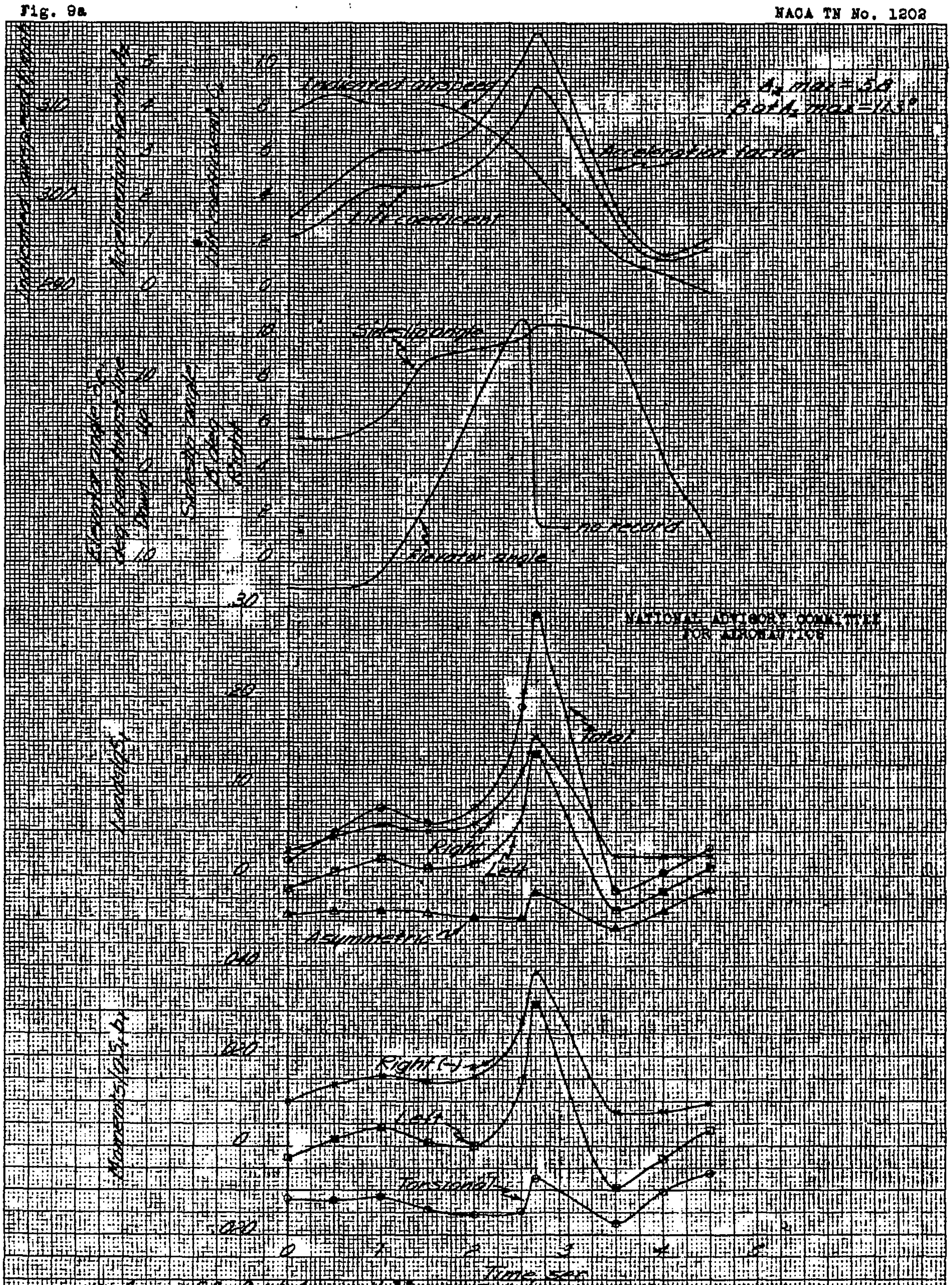

(a) $A_{z_{max}}$, 5.8; β at $A_{z_{max}}$, 11.3°.

Figure 9.- Time histories of power-off sideslipping dive pull-outs at approximately 290 miles per hour.

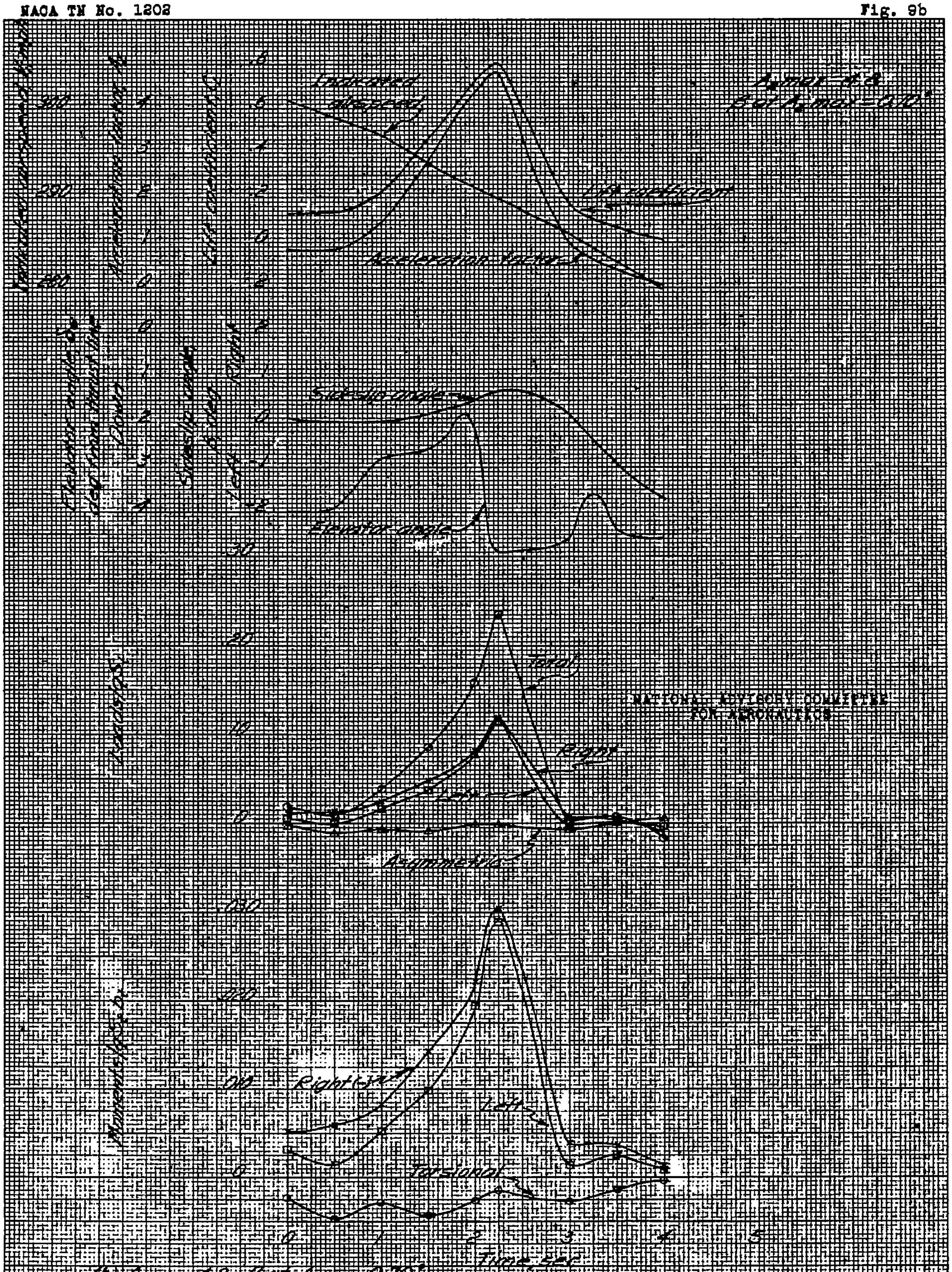

(b) $A_{z_{max}}$, 4.8; β at $A_{z_{max}}$, 0.70°.

Figure 9.- Continued.

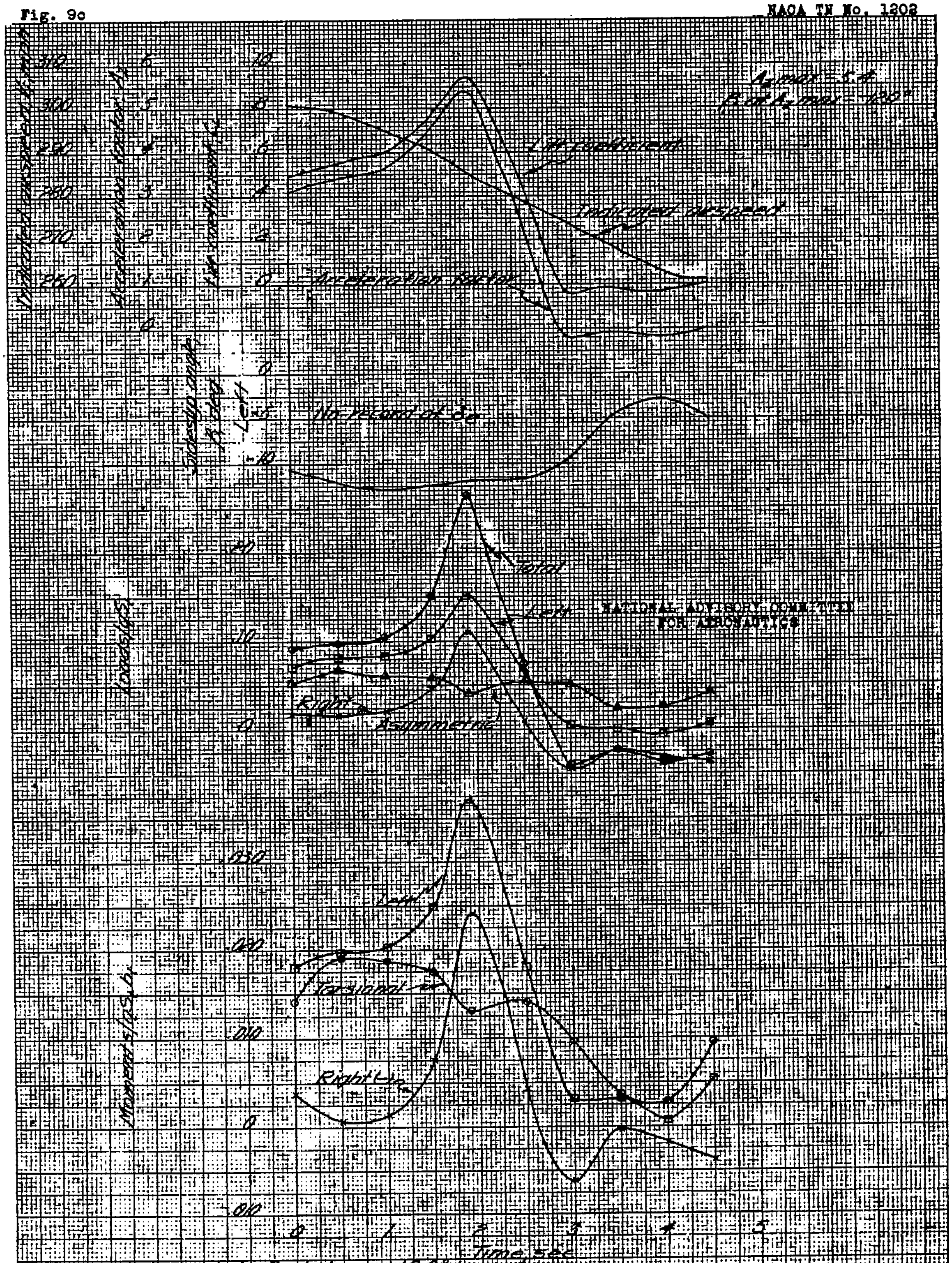

(c) $A_{z\,max}$, 5.4; β at $A_{z\,max}$, 12.0°

Figure 9.- Concluded.

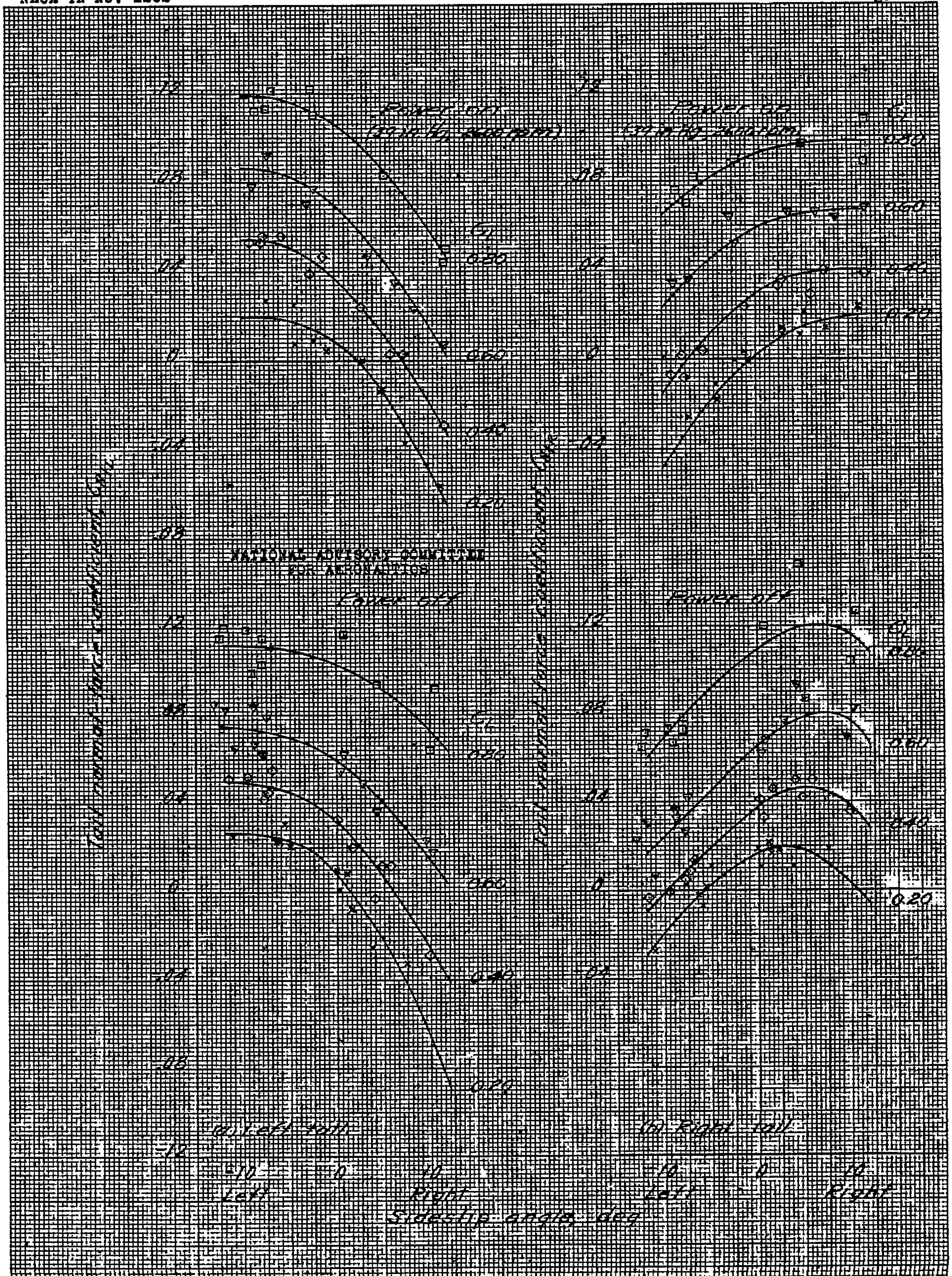

Figure 10.- Variation of tail normal-force coefficient with sideslip angle at several values of airplane lift coefficient. V_i, 290 mph; h_p, 5,000 ft.

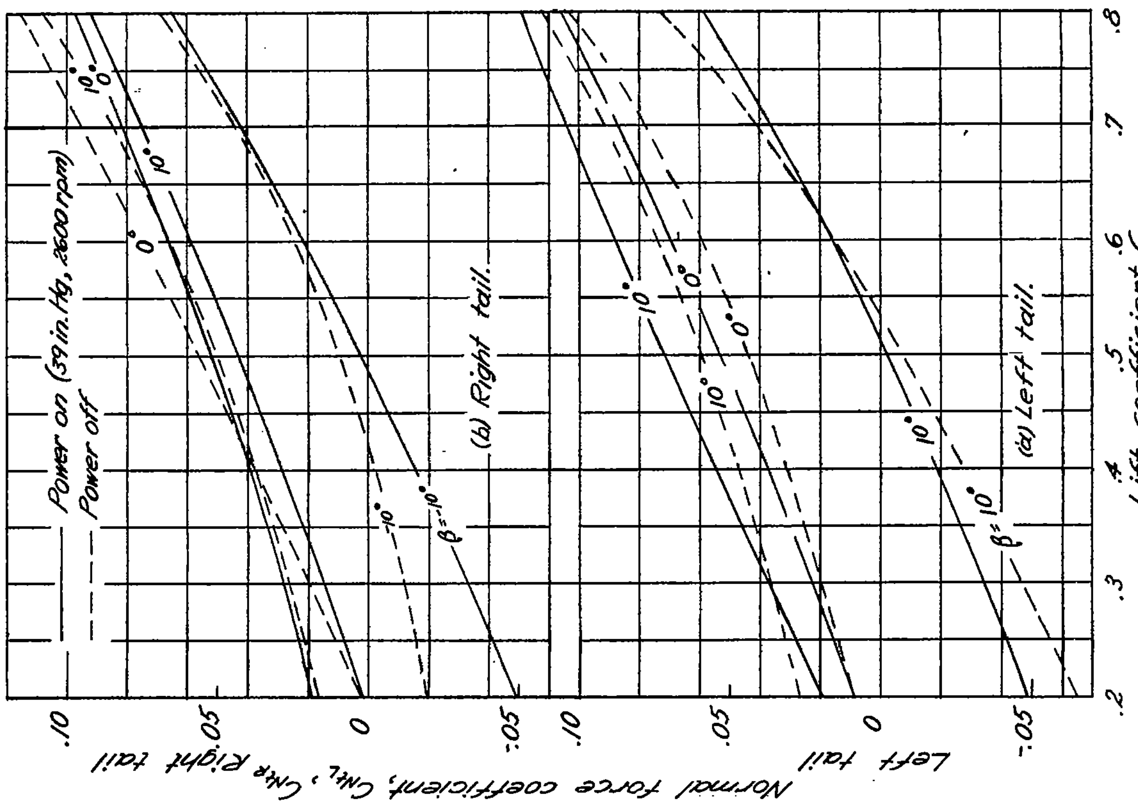

Figure 11. – Variation of $C_{N_{t_L}}$ and $C_{N_{t_R}}$ with C_L for several values of β. V_i, 290 mph; h_p, 15,000 ft.

NATIONAL ADVISORY COMMITTEE
FOR AERONAUTICS

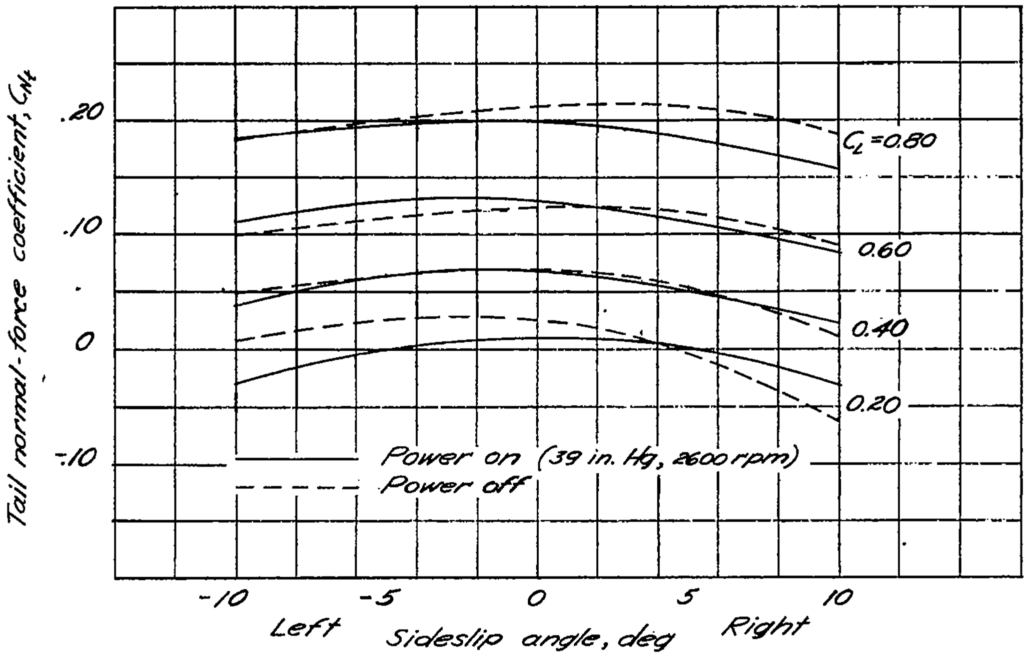

Figure 12. – Variation of total tail normal-force coefficient with sideslip angle at several values of airplane lift coefficient. V_i, 290 mph; h_p, 15,000 ft.

NATIONAL ADVISORY COMMITTEE
FOR AERONAUTICS

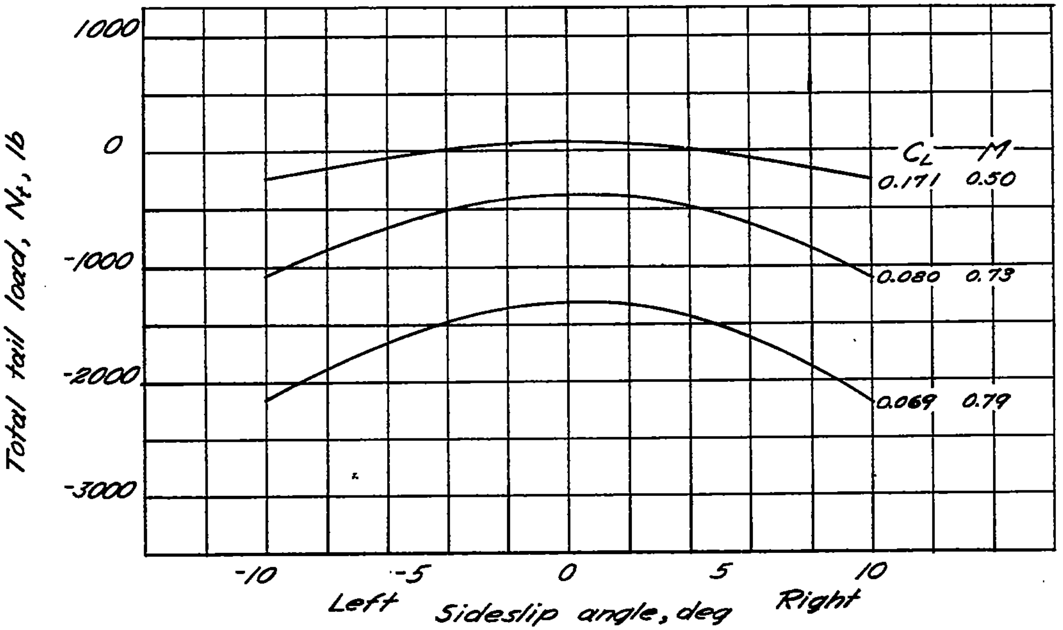

Figure 13.- Variation of total tail load with sideslip angle for various steady unaccelerated flight conditions. Power on. h_p,15,000 feet.

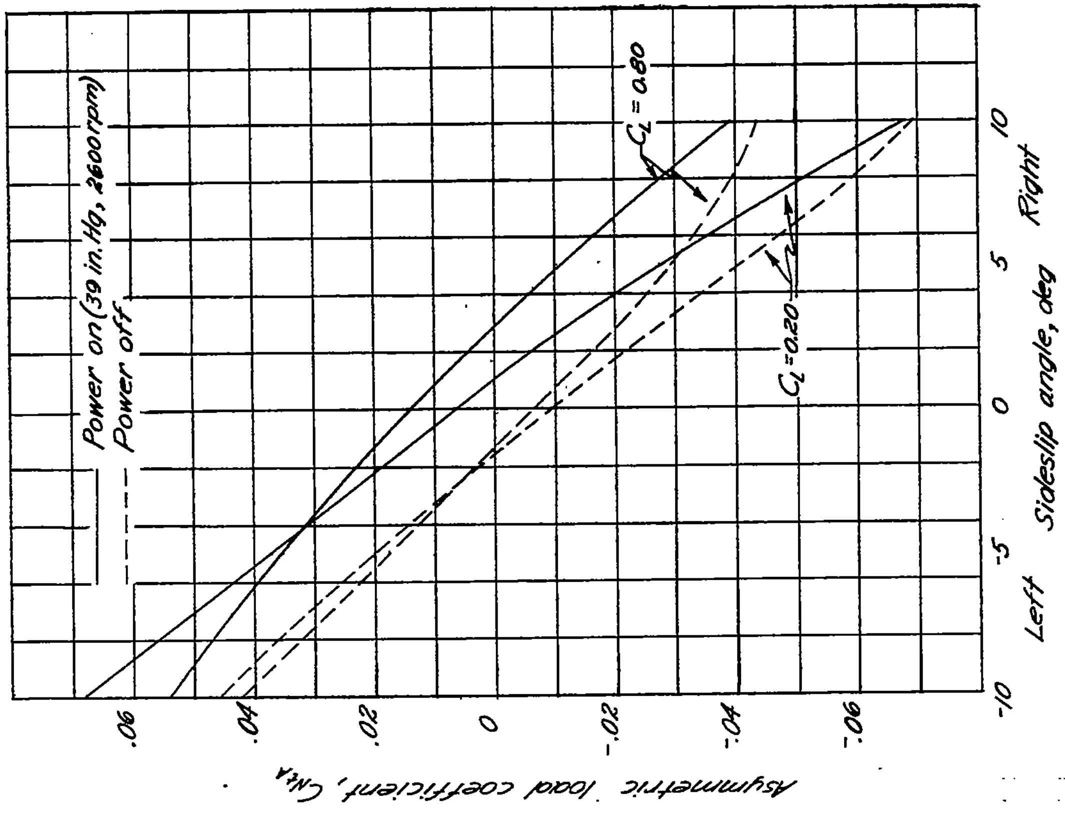

Figure 14.- Variation of asymmetric-load coefficient with sideslip angle at two values of airplane lift coefficient. V_i, 290 mph; h_p, 15,000 ft.

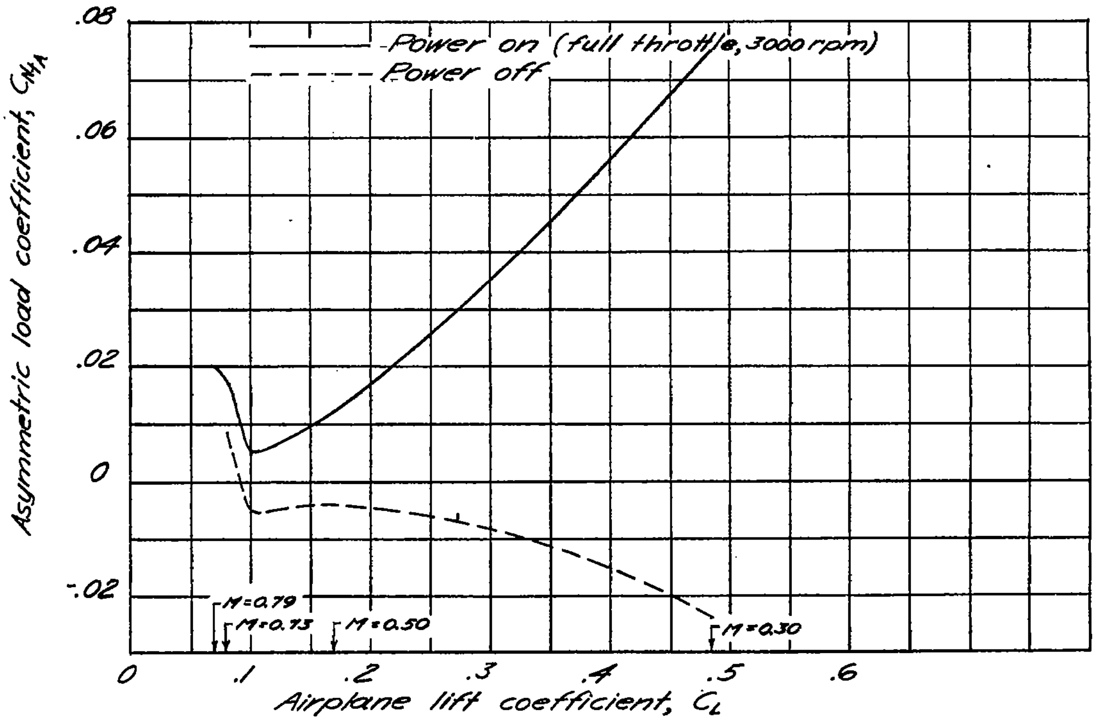

Figure 15.– Asymmetric-load coefficient in steady unaccelerated flight at a pressure altitude of 15,000 feet.

NATIONAL ADVISORY COMMITTEE
FOR AERONAUTICS

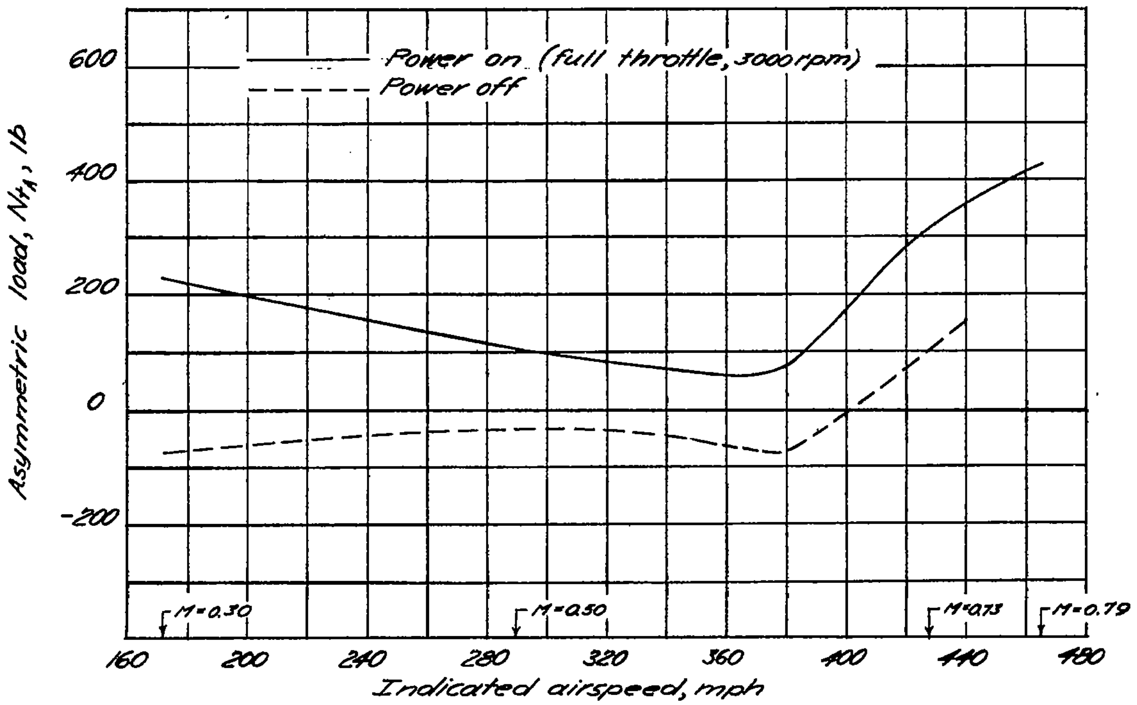

Figure 16. – Variation of asymmetric load with indicated airspeed at a pressure altitude of 15,000 feet. $A_z = 1.0$.

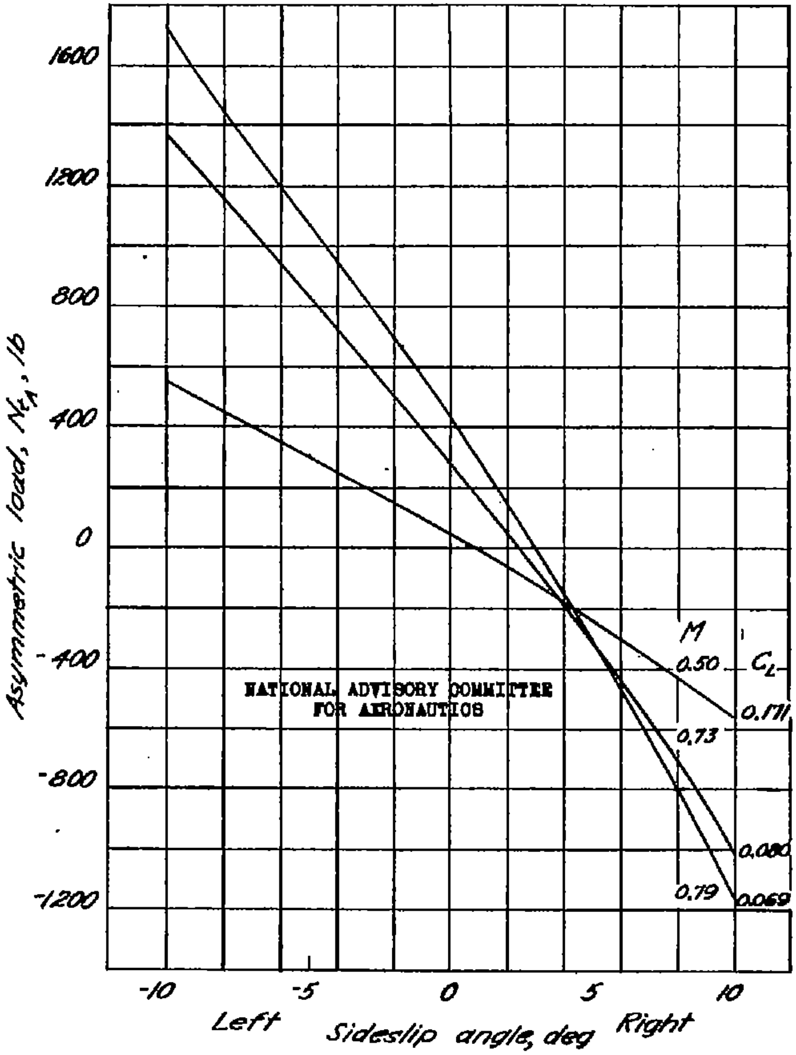

Figure 17.—Variation of asymmetric load with sideslip angle for various steady flight conditions. A_z = 1.0. Power on. h_p = 15,000 feet.

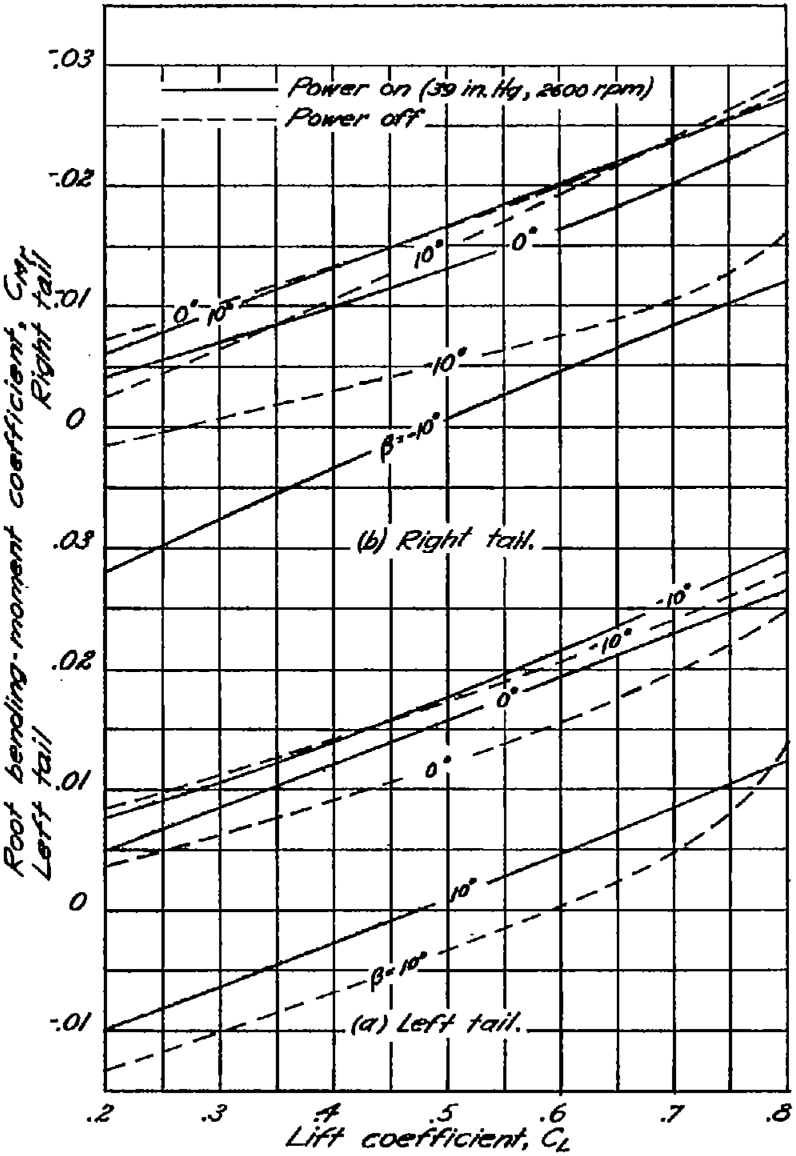

Figure 19.—Variation of $C_{M_{r_L}}$ and $C_{M_{r_R}}$ with C_L for several values of β. V_i, 290 mph; h_p, 15,000 ft.

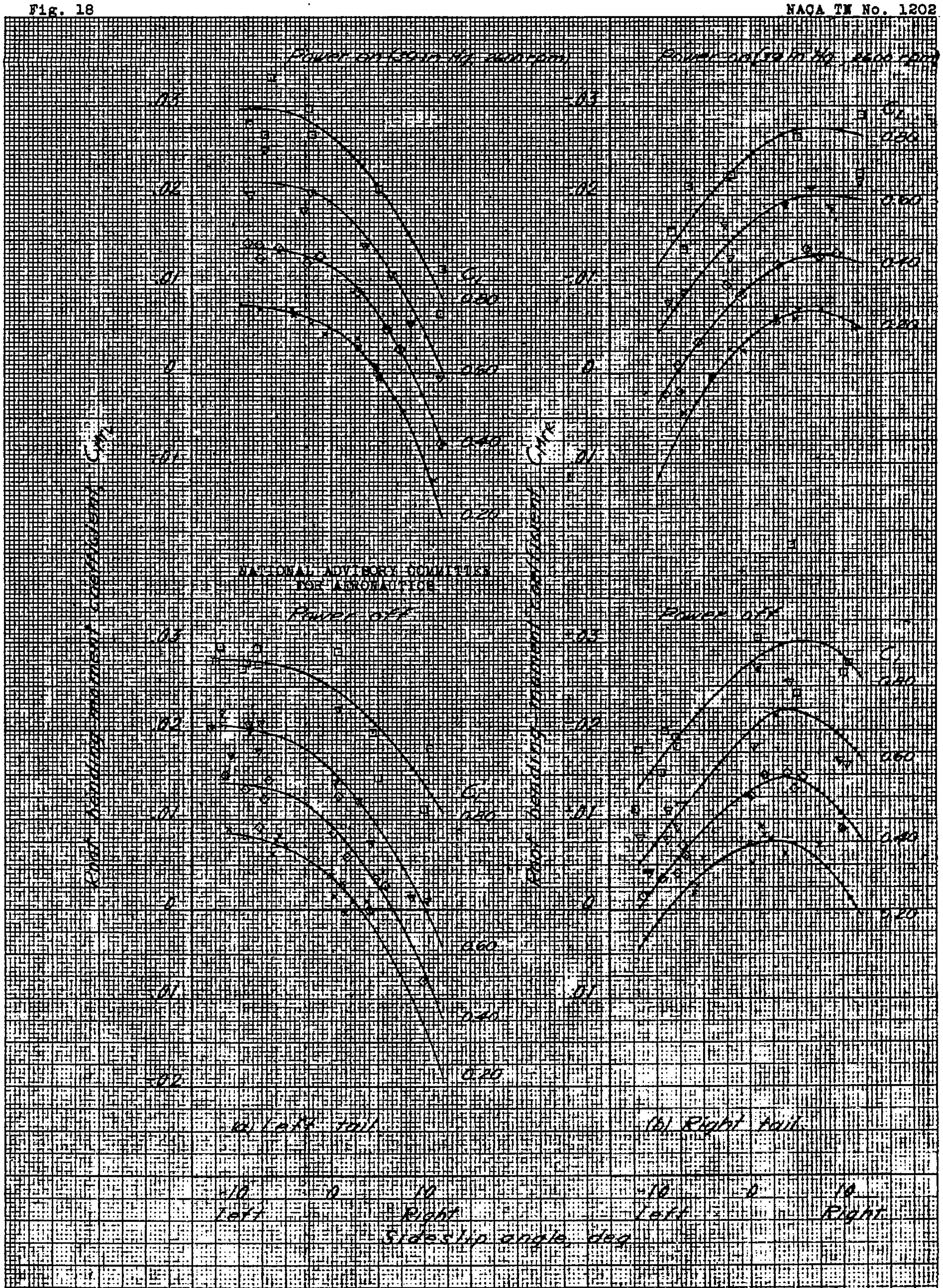

Figure 18.—Variation of root bending-moment coefficient with sideslip angle at several values of airplane lift coefficient V, 200 mph; hp, 5000 ft.

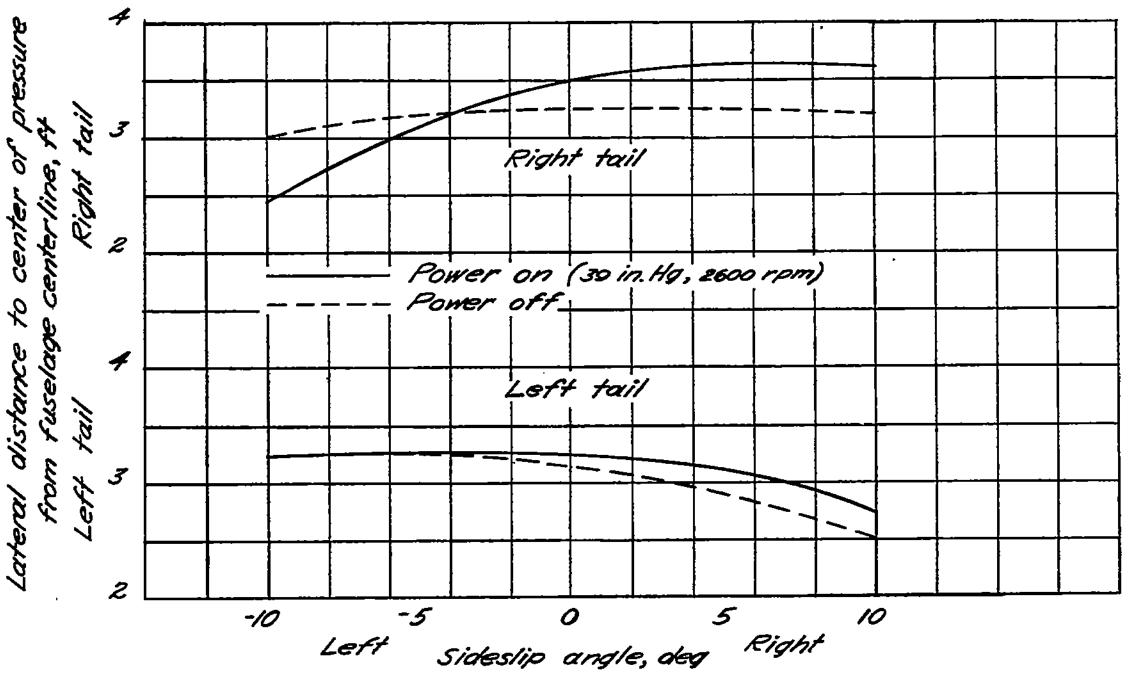

Figure 20.- Variation of lateral distance to center of pressure with sideslip angle at an airplane lift coefficient of 0.80. V_i, 290 mph; h_p, 15,000 ft.

NATIONAL ADVISORY COMMITTEE FOR AERONAUTICS

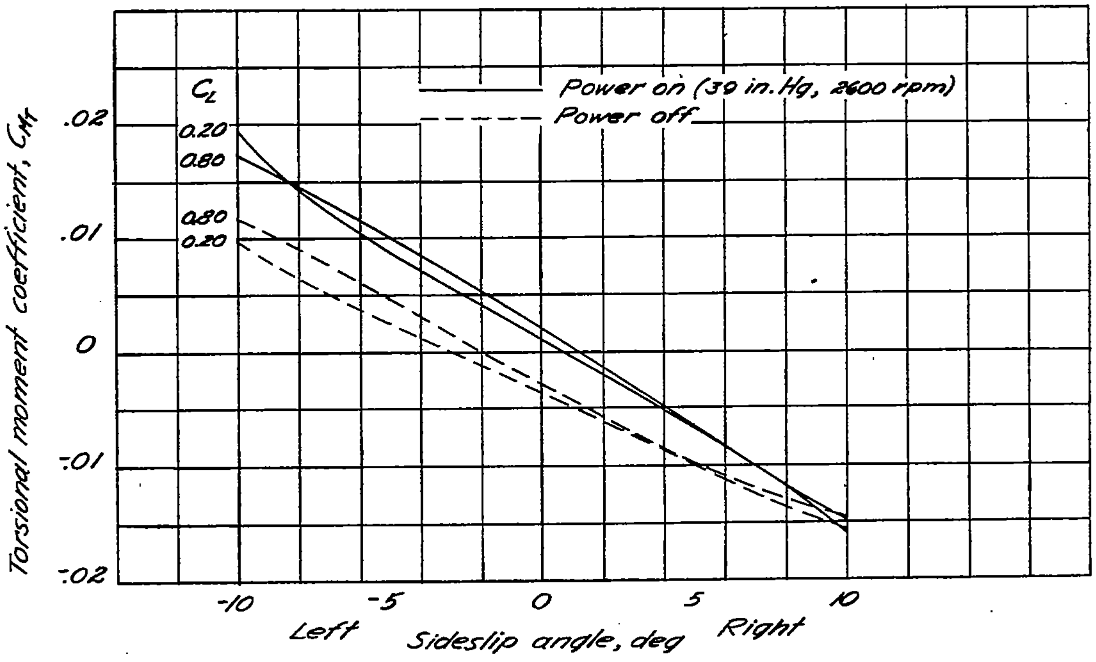

Figure 21. - Variation of torsional-moment coefficient with sideslip angle for two values of airplane lift coefficient V_i, 290 mph; h_p, 15,000 ft.

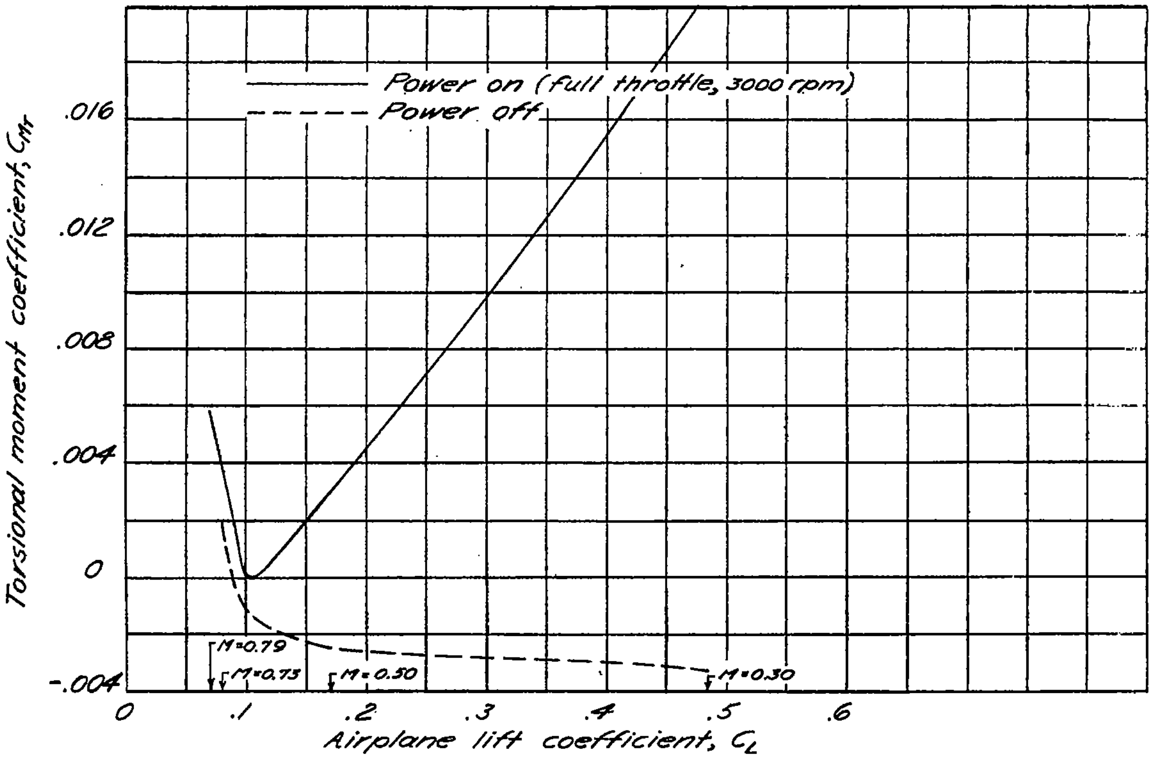

Figure 22.– Torsional moment coefficient in steady unaccelerated flight at a pressure altitude of 15,000 feet.

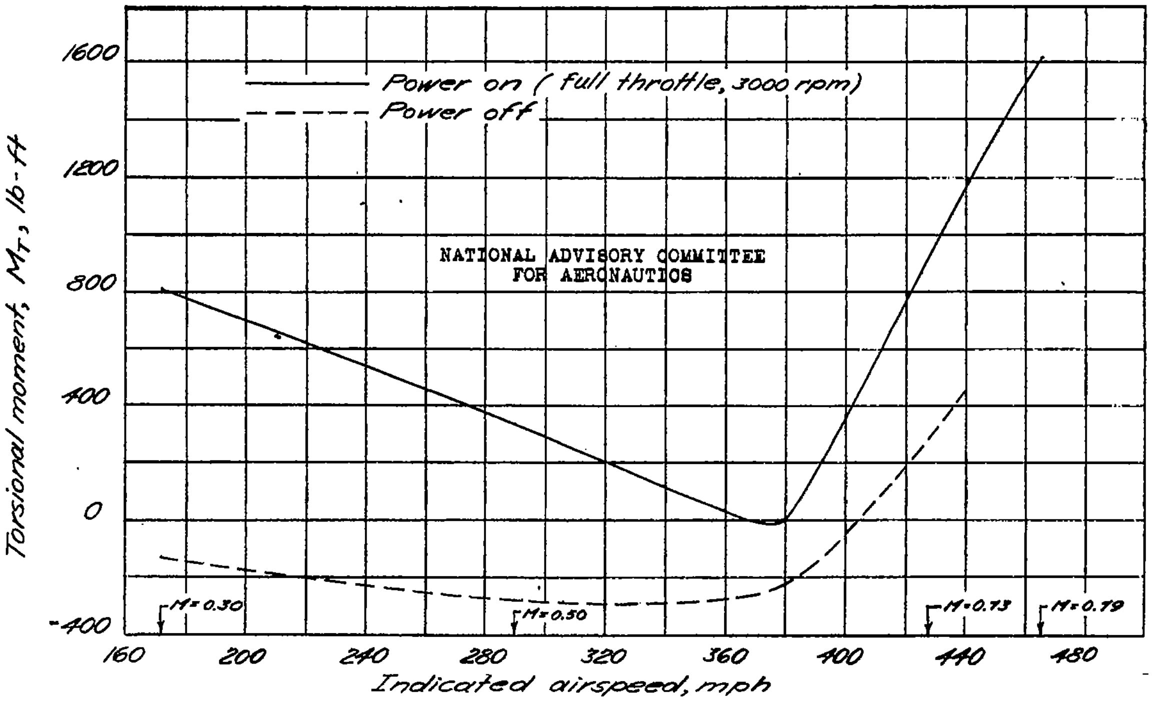

Figure 23.– Variation of torsional moment with indicated airspeed in steady unaccelerated flight at a pressure altitude of 15,000 feet.

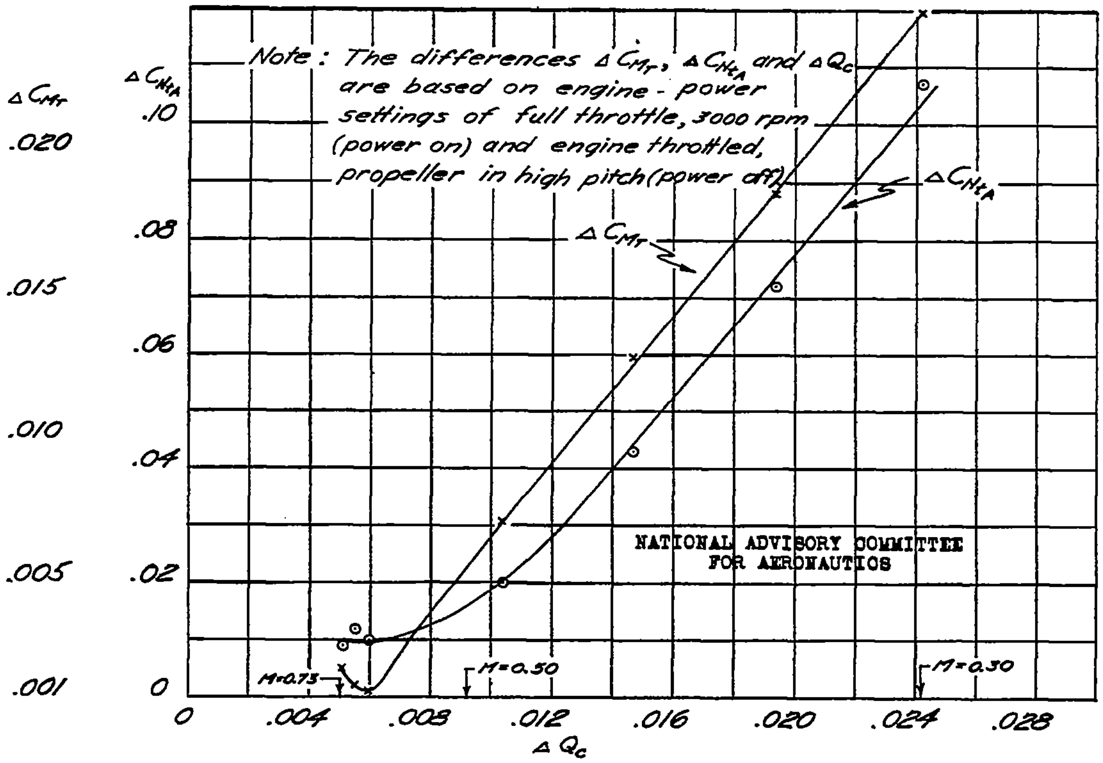

Figure 24. — Effect of torque coefficient on the asymmetric-load and torsional-moment coefficients in steady unaccelerated flight at a pressure altitude of 15,000 feet.

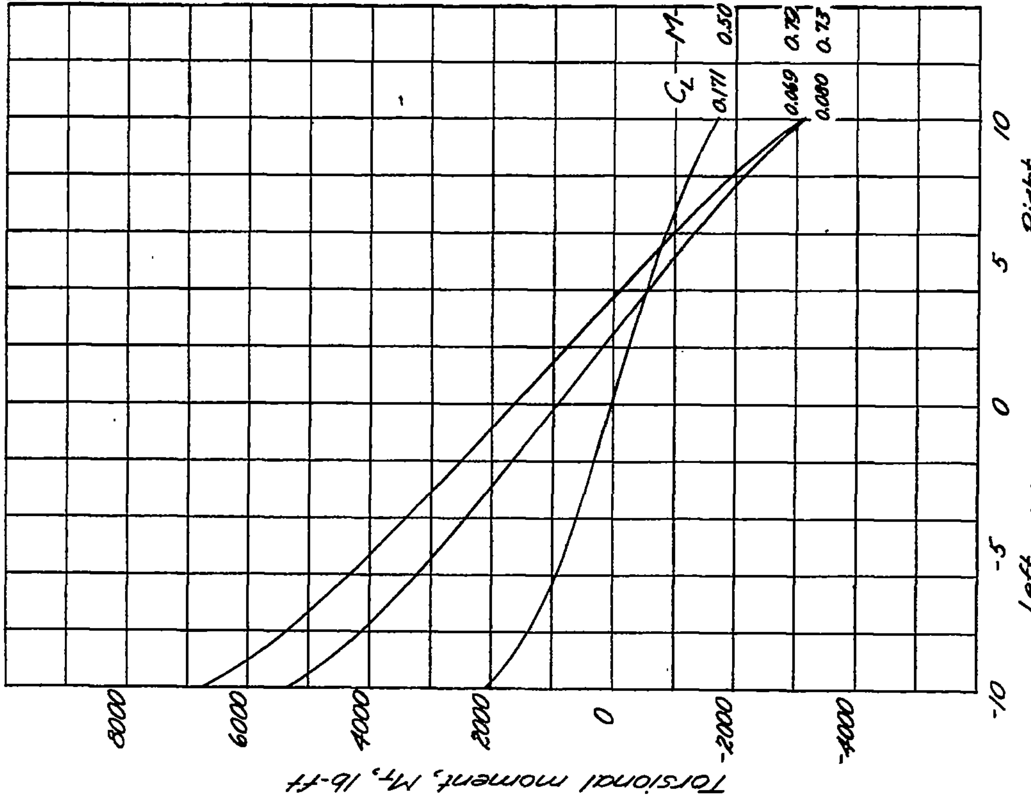

Figure 25. - Variation of torsional moment with sideslip angle for various steady flight conditions. $A_z = 1.0$, Power on. $h_p = 15,000$ feet.

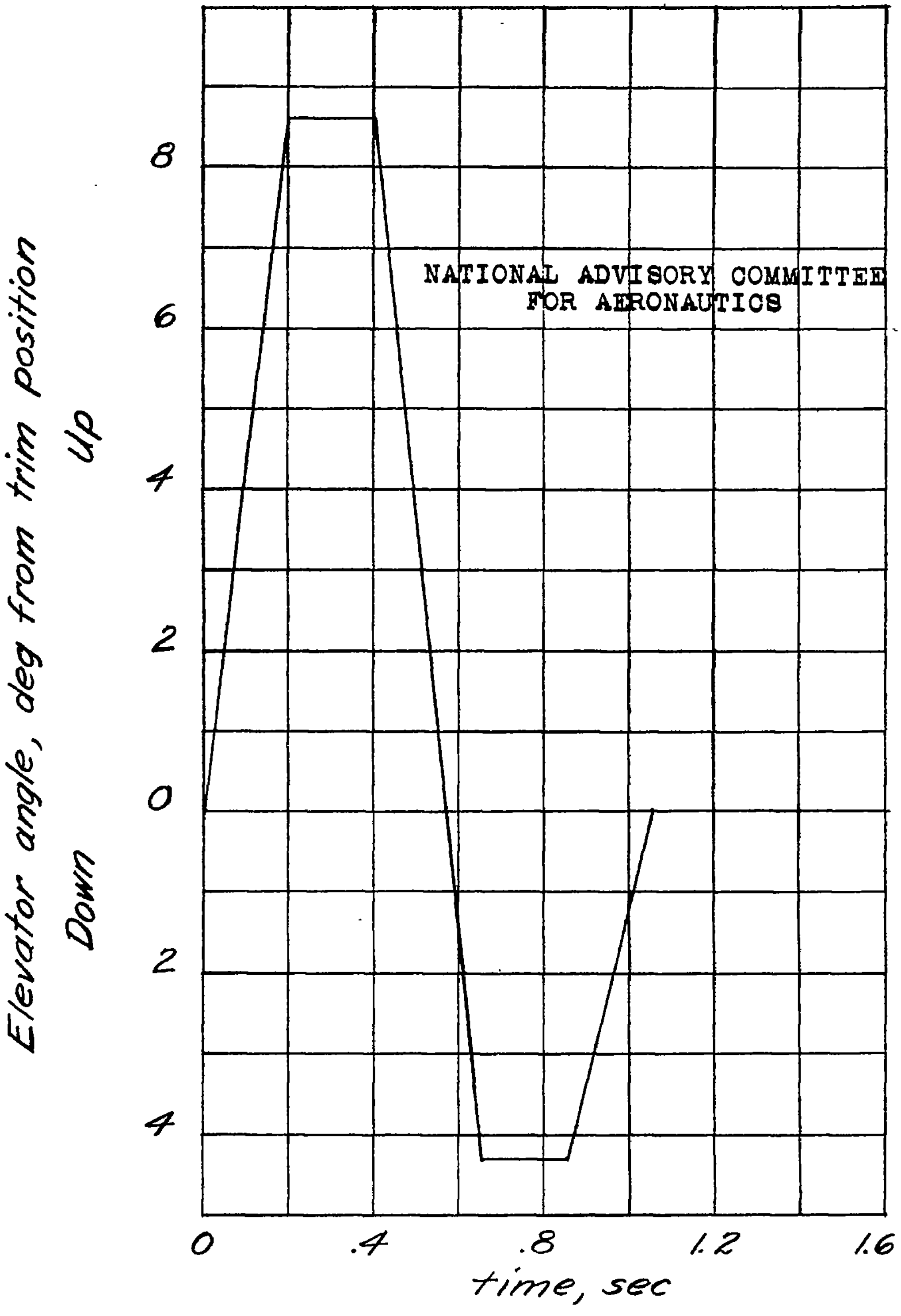

Figure 26. — Assumed elevator motion for calculating the maximum dynamic tail load.